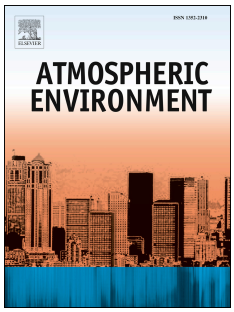

Pollutant concentrations and exposure variability in four urban microenvironments of London

Mamatha Tomson, Prashant Kumar, Gopinath Kalaiarasan, Juan C. Zavala-Reyes, Marta Chiapasco, Mark A. Sephton, Gloria Young, Alexandra E. Porter

PII: S1352-2310(23)00050-X

DOI: https://doi.org/10.1016/j.atmosenv.2023.119624

Reference: AEA 119624

To appear in: *Atmospheric Environment*

Received Date: 7 September 2022

Revised Date: 13 January 2023

Accepted Date: 27 January 2023

Please cite this article as: Tomson, M., Kumar, P., Kalaiarasan, G., Zavala-Reyes, J.C., Chiapasco, M., Sephton, M.A., Young, G., Porter, A.E., Pollutant concentrations and exposure variability in four urban microenvironments of London, *Atmospheric Environment* (2023), doi: https://doi.org/10.1016/j.atmosenv.2023.119624.

Author credits

Mamatha Tomson: Conceptualisation, Writing - original draft, Methodology, Validation, Visualisation, Writing - review and editing; **Prashant Kumar:** Conceptualisation, Investigation, Methodology, Project administration, Resources, Supervision, Visualisation, Writing - Original Draft, Writing - review and editing. **Gopinath Kalaiarasan:** Data Collection; Writing - review and editing. **Juan C. Zavala-Reyes:** Writing - review and editing; **Marta Chiapasco:** Data Analysis; Writing - review and editing; **Mark A. Sephton**: Writing - review and editing; **Gloria Young**: Data Analysis; Writing - review and editing; **Alexandra E. Porter**: Data Analysis; Writing - review and editing, Funding acquisition.

Graphical Abstract

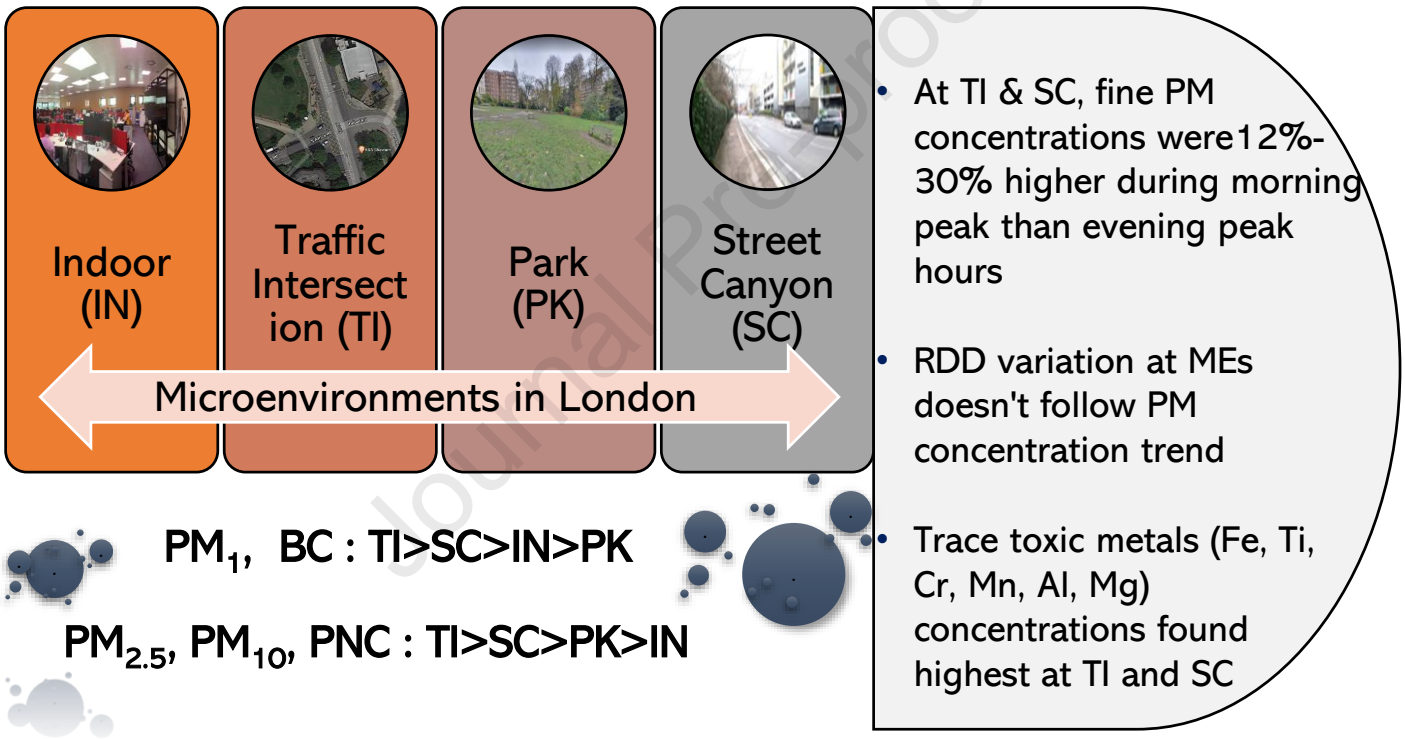

Pollutant concentrations and exposure variability in four urban microenvironments of London

Mamatha Tomson[a,e], Prashant Kumar[a,b,c,d,1], Gopinath Kalaiarasan[a], Juan C. Zavala-Reyes[a,f], Marta Chiapasco[h], Mark A. Sephton[g], Gloria Young[h], Alexandra E. Porter[h]

[a]*Global Centre for Clean Air Research (GCARE), School of Sustainability, Civil and Environmental Engineering, Faculty of Engineering and Physical Sciences, University of Surrey, Guildford GU2 7XH, Surrey, United Kingdom*

[b]*Institute for Sustainability, University of Surrey, Guildford GU2 7XH, Surrey, United Kingdom*

[c]*Department of Civil, Structural & Environmental Engineering, Trinity College Dublin, Dublin, Ireland*

[d]*School of Architecture, Southeast University, Nanjing, China*

[e]*SMART Infrastructure Facility, Faculty of Engineering and Information Science, University of Wollongong, Wollongong 2522 NSW, Australia*

[f]*Escuela Nacional de Estudios Superiores–Mérida, Universidad Nacional Autónoma de México, 97357 Mérida, Yucatán, México*

[g]*Department of Earth Science and Engineering, Prince Consort Road, Imperial College London, SW72AZ*

[h]*Department of Materials, Prince Consort Road, Imperial College London, SW72AZ*

[1] Corresponding author. Address as above. E-mail addresses: p.kumar@surrey.ac.uk, prashant.kumar@cantab.net

Abstract

We compared various pollutant concentrations (PM_1, $PM_{2.5}$, PM_{10}, PNC, BC) at four different urban microenvironments (MEs) in London (Indoor, IN; Traffic Intersection, TI; Park, PK; and Street Canyon, SC). The physico-chemical characteristics of particles were analysed, and the respiratory deposition doses (RDD) were estimated. Field measurements were conducted over a period of 121 days. The mean $PM_{2.5}$ (PNC) concentrations were found to be 9.47±7.05 (16366±11815), 8.09±4.57 (10951±6445), 5.11±2.96 (7717±4576), 3.88±3.06 (5672±2934) μg m^{-3} (# cm^{-3}) at TI, SC, PK and IN, respectively. $PM_{2.5}$, PM_{10} and PNC exhibited a trend of TI>SC>PK>IN; higher concentrations for PM_1 and BC were observed at IN than PK due to the emissions from printers, producing a trend of TI>SC>IN>PK. We observed 12%-30% higher fine PM concentrations at TI and SC sites during morning peak (07:00-09:30) than the evening peak hours (16:00-19:00); while IN showed a smaller variation in fine PM concentrations compared with outdoor TI, PK and SC sites owing to their prevalence in the IN for a longer time. Fine and ultrafine PM containing potentially toxic trace transition metals including Fe, Ti, Cr, Mn, Al and Mg were detected by high resolution electron microscopy at all sites. There was a similar relative abundance of different elements at the TI, IN and PK sites, which suggests a transport of PM between MEs. RDD for PM_1 was highest (2.45±2.27 μg h^{-1}) at TI for females during running; $PM_{2.5}$ and PM_{10} were highest at SC (11.23±6.34 and 37.17±20.82 μg h^{-1}, respectively). The results show that the RDD variation between MEs does not follow the PM concentration trend. RDD at PK was found to be 39%-53% lower than TI and SC during running for all the PM fractions. Overall, the study findings show the air quality variation at different MEs and reveals the exposure inequalities around the city, which enable the management of personal exposure by selecting appropriate MEs for different activities.

Keywords: Urban microenvironment; Air quality; Diurnal variation; Particulate matter; Chemical composition; Human exposure

1. Introduction

Ambient air pollution in both cities and rural areas was estimated to cause 4.2 million premature deaths worldwide in 2016 (WHO, 2018). Air pollutants constitute a complex mixture originating from vehicular emissions, coal combustion and can be from secondary pollution (Kumar et al., 2011a). Policies and investments to reduce sources of outdoor air pollution have been taken by many countries. Particulate matter (PM) is a portion of air pollution that is made up of small particles and liquid droplets containing soot aggregate, secondary organic aerosols, nitrates, sulfates, soil or dust, bioaerosols as well as different trace transition metals (Anderson et al., 2012). Different sources contribute to fine ($PM_{2.5}$; ≤2.5μm in aerodynamic diameter) and coarse particles ($PM_{2.5-10}$; between 2.5 and 10 μm) in different microenvironments (MEs). Motor vehicles are major contributors to urban air pollution (Kaur et al., 2005), contributing both primary PM and also noxious gases such as nitrogen dioxide (NO_2) and volatile organic compounds (VOCs) including polycyclic aromatic hydrocarbons (PAHs) (Hama et al., 2017). Fine particles mostly originate from partial combustion of fuel in engines and coarse particles come from non-exhaust vehicular sources (Harrison et al., 2001; Thorpe and Harrison, 2008). PM with aerodynamic diameters <100 nm are called ultrafine particles (UFP), which are abundant in number but contribute little to the total mass (Berghmans et al., 2009). Dominant sources of UFPs are direct emissions from motor vehicles and secondary particles generated by photochemical or physical processes in the atmosphere (Berghmans et al., 2009; Fine et al., 2004). High concentrations and long-term exposure to $PM_{2.5}$ are associated with increased pulmonary and cardiovascular mortality (Anderson et al., 2012; Spinazze et al., 2013) and $PM_{2.5-10}$ also affects mortality

(Puett et al., 2009). UFPs are more toxic than larger PM since they get deposited in the bronchioles and alveoli (Berghmans et al., 2009) and can translocate into the bloodstream (Heinzerling et al., 2016; Qvarfordt et al., 2022).

People move into different MEs in urban areas during their day-to-day life, with different levels of pollution. Assessment of human exposure in different MEs is of great interest as it leads to improved understanding on exposure mitigation and to generate recommendations that protect public health. The variation in concentrations and composition of atmospheric pollutants between different MEs are related to the sources of urban pollutants, seasons, day and time (Spinazze et al., 2015); and the personal exposure varies with proximity to the sources (Spinazze et al., 2013) and with the activity patterns among population groups (Lim et al., 2012). Table 1 summarises the previous studies that have investigated pollutant concentrations along with chemical composition, and personal exposure in different MEs, and describes the chemical composition. (Lonati et al., 2010; Jones et al., 2000; Harrison et al., 2004; Spinazze et al., 2015).

Traffic intersections (TIs) are a significant hotspot in urban areas, showing particle number concentration (PNC) - defined as the number of particles per unit volume of air and a measure of UFPs - 17-times higher than average roadside PNCs (Goel and Kumar, 2014). Street canyons are another most polluted urban microenvironment with accumulation of air pollutants due to limited dispersion of traffic emissions (Abhijith et al., 2017). Street canyon geometry, traffic characteristics, atmospheric stability, and turbulence induced by prevailing winds also affects the pollutant concentration in a street canyon (Tomson et al., 2021; Voordeckers et al., 2021). Areas without major influences of local roads or point sources are considered to represent the urban background air quality (Bigi and Harrison, 2010; Birmili et al., 2016; Luengo-Oroz et al., 2019).

Simultaneous measurements exhibited a high temporal variation for PNCs at street level compared with urban background sites (Boogaard et al., 2010). A study in Italy showed highest pollutant exposures to UFPs near motorised traffic and lowest in a park (Cattaneo et al., 2009). Similarly, studies in London and Birmingham reported higher PM concentrations in urban roadsides compared to urban and rural backgrounds and are composed of elemental carbon, organic compounds and iron-rich dusts (Harrison et al., 2004: Yin and Harrison, 2008). In other works, highest pollutant concentrations occurred at TIs and roadsides, and the least at parks (Brzozowski eta l., 2019; Piotrowicz and Polednik, 2019; Spinazze et al., 2015; Kumar et al., 2021). However, little is known about the composition and structure of the fine or ultrafine PM in these environments owing to the challenge of characterising micro to nanometer-sized particles. It is important to address this knowledge gap as $PM_{2.5}$ can become internalised by cells and cause damage to intracellular organelles (Miao et al., 2019).

Indoor air quality is also a major concern as this is where most people spend the majority of their time (Miller et al., 2017; Shrestha et al., 2019). Indoor MEs (both residential and non-residential) are the larger contributors to personal exposure compared to transportation and outdoor environments (Lim et al., 2012). The concentration and type of pollutant depends on the proximity of the indoor environment to congested roads alongside building characteristics such as penetration factor, ventilation and infiltration (Miller et al., 2017). Indoor PM levels vary also based on variation in air exchange rates and various indoor activities (Jones et al., 2000; WHO, 2018; Kumar et al., 2022a).

Previous studies (Table 1) have assessed mostly variability of a single pollutant (e.g. PNC in Cattaneo et al., 2009) or specific fraction of PM (e.g. $PM_{2.5}$ in Kaur et al., 2005). Others have focused on the analysis of the variation of exposure to UFPs with different fractions

of PM (e.g., Harrison and Jones, 2005; Borsós et al., 2012) or assessed the personal exposure of people in urban transport MEs in the UK (Rivas et al., 2017b; Kaur et al., 2005). However, limited studies have been performed comparing different urban MEs, particularly including indoor environments; none of which examined UFP counts, composition and morphology, along with other PM components (PM_1, $PM_{2.5}$ and PM_{10}) and potential personal exposure (Table 1), due to the practical inconvenience of conducting continuous air quality monitoring in different MEs.

The overall objective of this work is to acquire integrated measurements of PNC, size-resolved PM concentration (PM_1, $PM_{2.5}$ and PM_{10}) and black carbon (BC) along with CO and CO_2 as co-pollutants at four sites along with the characterisation of the diameter, morphology and composition (trace metal and PAHs) of $PM_{2.5}$ and their nanoscale substructures. Field measurements were performed to assess the air pollution at four different MEs - indoor (IN), traffic intersection (TI), park (PK) which is an urban background site, and a street canyon (SC). We quantified pollutant concentrations in each ME, to extend our knowledge of the variability in pollutant concentrations and to calculate human exposure to different pollutants in these MEs. To identify the potential sources of the PM and their potential health impacts, we surveyed multiple indicators in each ME that included diurnal concentration variations of PMs with different size distributions, and characterisation of the morphology, and composition of the respirable fraction of $PM_{2.5}$. This multidisciplinary approach enabled us to generate indicators that fingerprint the potential sources of the PM. The specific aims were to: (i) quantify air pollutant concentration variations in different urban MEs, (ii) evaluate the diurnal variation of those pollutants, (iii) compare the PM fractional ratios at different MEs, (iv) characterise the morphology and chemistry of metals in individual fine and ultrafine PM pollutants and compare the composition and size distribution of the potentially most toxic

components, and (v) provide insight into the exposure assessment in terms of respiratory deposition doses (RDD).

2. Materials and methods

2.1 Site description

Monitoring of airborne concentrations of pollutants was carried out at four different sites (Figure 1) in London to represent various MEs (IN, TI, PK and SC). Different air quality monitoring instruments were used to estimate the pollutant concentrations and to collect the particles on filters. The IN measurements were carried out in the Data Science Institute (DSI; William Penney Laboratory) located at South Kensington (latitude: 51.4989, longitude: -0.1771). The office room in DSI has a floor area of 168.53 m^2, where nearly 15 people used to work (8 to 10 hours) during the campaign period. The TI measurements were carried out at the 4-way TI in front of The Invention rooms located at White city (latitude: 51.5128, longitude: -0.2251), where South Africa road, Depot road and Wood lane road intersect. The TI is 130 m from White city and 350 m from Wood lane underground stations.

The PK site measurements were carried out in Secret Gardens (Princes Gate Garden) located at Knightsbridge (latitude: 51.5005, longitude: -0.1721). The park is located within an urban area that is not close to busy streets, representing an urban background site. The studied SC site was across the Du Cane road at White City (latitude: 51.5164, longitude: -0.2335), which is a shallow canyon having an aspect ratio (*H/W*) of 0.42 (Tomson et al., 2021), and an average traffic volume of 650 vehicles $hour^{-1}$ during the daytime (Kumar et al., 2022b). None of the measurement sites were near industrial areas, large parking areas or gas stations.

2.2 Instrumentation

We monitored PM_{10}, $PM_{2.5}$, $PM_{1,}$ PNC, CO, CO_2 and BC concentrations in each MEs. All the instruments used for pollutant monitoring were connected to a continuous electric power supply. GRIMM (model 11-C) optical aerosol monitor (GRIMM Technologies Inc., Germany) measured PM_1, $PM_{2.5}$, PM_{10}. It captures airborne particles from a size range of 0.25-32 μm diameter, with a sensitivity of 0.1 μg m^{-3} and is classified in 31 different size channels. We measured PM concentration with a sampling frequency of 1 min in all the measurement sites, at a flow rate of 1.21 L min^{-1}. P-TRAK 8525 (TSI Inc., USA) was employed to measure PNC in the size range of 0.02–1 μm in the 0 to $5x10^5$ particles cm^{-3} concentration range. We measured PNC every 1 min with a flow rate of 0.71 L min^{-1}.

Q-TRAK 7575-X (TSI Inc., USA) was employed to measure temperature, relative humidity, barometric pressure and CO, CO_2 concentrations in the ambient air, at a logging interval of 1 min. Q-TRAK measures CO_2 in the range of 0 to 5000 ppm and CO between 0 to 500 ppm. These instruments have been widely used for pollutant concentration measurements in various previous studies (Kumar et al., 2022b; Abhijith and Kumar, 2019; Rivas et al., 2017a; Sharma and Kumar, 2020). BC concentrations were collected using a portable MicroAeth M200 (Aethlabs, USA). MicroAeth measures the mass concentration of light absorbing carbonaceous particles in a sampled aerosol. It provides BC concentrations derived from measurements of the rate of change in absorption of transmitted light at 880 nm due to continuous collection of aerosol deposits on the filter. During the monitoring period, the time base was set to 1 min at a flow rate of 0.1 L min^{-1} to minimise the filter loading. The instrument has a measurement accuracy of ± 0.1μg BC m^{-3} and a detection limit of 30 ng BC m^{-3}. Filter cassette in microAeth was changed as required when it was getting saturated. Attenuation in BC data generated due

192 to instrumental optical and electronic noise is rectified by post-processing the data with
193 the optimised noise-reduction averaging algorithm (Hagler et al., 2011).

194 **2.3 Data collection and processing**

195 Fieldwork was carried out over a total of 121 days between 25 November 2019
196 and 22 September 2020 at four different MEs as detailed in Table 2. All the instruments
197 were logging continuously at IN and PK sites, except P-TRAK, producing continuous
198 data over the 24 hours on most days. P-TRAK was logging only during the daytime, due
199 to the inconvenience of changing the alcohol wick in the night. At TI and SC sites, all the
200 instruments logged data during the daytime (07:00-19:00 h), because it was not feasible
201 to run the equipment unattended during the night-time for the health and safety of on-site
202 researchers and the risk of vandalism. All the intercomparisons were made on the
203 harmonised pollutant concentrations dataset over the same monitored period (07:00-
204 19:00 h). At the IN site, all the instruments were kept in a table at one of the corners of
205 the office space (SI Figure S1).
206 At the TI site, the samplers were placed inside the compound wall of a nearest building,
207 at 4 m from the side of the road. Meteorological data (wind speed (WS), temperature,
208 relative humidity) were obtained from Heathrow airport (51.4700, -0.4542), which is
209 located 15 km away and represents the meteorological conditions in the measurement
210 sites (SI Table S1). The same meteorological station data was used in previous studies
211 (Chapman et al., 2017; Kolokotroni et al., 2007). The wind rose patterns are presented in
212 Supplementary Information, SI, Figure S2. Traffic counting was performed manually
213 during different periods of measurement (between 07:00h and 19:00h) in the TI site, by
214 categorising the vehicles as two wheelers, cars, bus, LDV and HDV, which was then
215 extrapolated to measure hourly average traffic volume (SI Figure S3). The average traffic
216 volume on the road during the measurement period was 1300 vehicle hour^{-1}. SC site has

pavements of 3 m width along the road on both sides, on which the instruments were kept (SI Figure S1), mounted on a tripod stand at 1.5 m heigh. Field measurements were not carried out on rainy and windy days considering the safety of the instruments, variation in measurements and difficulty in attending monitoring. All the instruments (Section 2.2) used for the monitoring were calibrated prior to measurements.

All the air pollutant concentration data collected were cleaned and analysed using Microsoft Excel and R statistical software (v4.0.3) (R Core Team, 2020) and the openair package (Carslaw and Ropkins, 2012). Box plots, windrose diagrams, time plots as well as diurnal variation plots were produced for different pollutant data to investigate the pollutant variations in different MEs. PM data was further used to calculate $PM_1/PM_{2.5}$ and $PM_{2.5}/PM_{10}$ ratios. RDD calculations performed using Microsoft Excel.

2.4 Estimation of RDD

We quantified the variations in RDD for different PM fractions during different physical activities by adults and children at various MEs. The RDD at each ME was calculated using Eq. (1), which is adapted from ICRP (1994) and following the methodology described in previous works (Kumar and Goel, 2016; Rivas et al., 2017b; Abhijith and Kumar, 2021). The RDD values are expressed in terms of mass of particles deposited per unit time (μg h^{-1}). RDD is the product of particle mass concentration (PMC), deposition fraction (DF) and ventilation rate (VR). The PMC varies in different MEs, DF is influenced by particle size and is proportional to mass median diameter (d_p, μg) of PM fractions, VR depends on age, sex and the activity of a person.

$$RDDi = DFi \times PMi \times VR_j \quad (1)$$

Where i represent different PM fractions (PM_1, $PM_{2.5}$, PM_{10}); DF_i and PM_i represent DF and PMC for each of the PM fractions. VR is the ventilation rate for the j^{th} individual;

241 DFs are calculated using Eq. (2) and (3), presented in Hinds (1999). d_p was found out by
242 reading the particle diameter corresponding to a cumulative percentage of 50% PM mass,
243 following the method given in previous studies (Kumar et al., 2018, 2017; Kumar and
244 Goel, 2016; Rivas et al., 2017b; Abhijith and Kumar, 2021)

245 $$DF = IF\left(0.058 + \frac{0.911}{1+exp(4.77+1.485ln\ dp)} + \frac{0.943}{1+exp(0.508-2.58ln\ dp)}\right) \quad (2)$$

246 $$IF = 1 - 0.5\left(1 - \frac{1}{1+0.00076dp^{2.8}}\right) \quad (3)$$

247 The VRs for the exposure assessment during various activity levels were adopted from
248 US-EPA (2009).

249 **2.6 Particulate Characterisation**

250 Chemical and morphological characterisation of the PM collected on quartz filters
251 (from IN, TI, PK sites) was conducted using FEI Quanta scanning electron microscope
252 (SEM) and Jeol 2100F transmission electron microscope (TEM) combined with energy
253 dispersive x-ray spectroscopy (EDXS), using a Bruker XFlash 6/60 detector. The detailed
254 description of collection of particles on filters using MiniVol samplers and Harvard
255 impactors are given in SI Section S1. Elemental maps were processed using Feature
256 Analysis for Quantax Esprit 2.1 (Bruker, USA). The TEM data was analysed using the
257 Gatan Digital Micrograph and ImageJ (Schneider et al., 2012). EDXS maps were
258 collected in STEM mode using a dark field detector and the Oxford Instruments
259 INCA/Aztech EDS 80 mm X-Max detector system. Oxford Instruments AzTec software
260 was used to analyse the EDXS maps. Poly aromatic hydrocarbons were measured by gas
261 chromatography - mass spectrometry (GC-MS). Detailed method descriptions of the
262 electron microscopy, ICP-MS and GC-MS organic compound analysis are given in SI
263 Sections S2-S4.

3. Results and Discussion

3.1 Overview of pollutant concentrations in different MEs

Table 3 summaries the data availability, mean, median and standard deviation of pollutant concentration on each of the MEs during daytime (07:00-19:00 h). Mean meteorological parameters at the four measurement sites during the field measurement period are summarised in Table S1. Average temperature and relative humidity at SC were different from other two outdoor MEs as the SC measurements were carried out in the summer. As far as WS is concerned, the mean values were closer to each other. The highest mean WS was found at the TI site and the lowest was at SC during the measurement period (SI Figure S2). Figure 2 shows the pollutant concentrations at four MEs. The $PM_{2.5}$, PM_{10} and PNC exhibited a similar trend, showing least average concentration at IN and highest concentration at TI, followed by SC and PK. Common PM trends existed because the major emission sources of TI and SC are associated with road traffic. But PM_1 and BC concentrations are higher at IN than PK sites and displayed a trend of TI>SC>IN>PK.

The IN considered for this study is an office space in an academic institute (Section 2). The main sources of pollutants in the IN office environment are printers, copy machines, usual office activities (Setyawati et al., 2020), and the infiltration of pollutants from the outside (Section 3.5). These activities emit particles in a UFP size range similar to those characteristic of combustion processes which prevail in the IN environment for a longer time (Gomes et al., 2012). The average PNC value in the office space (5672±2934 cm^{-3}) was in the observed range seen in previous studies, even though it was slightly less than in most previous research (Spinazze et al., 2013; Cattaneo et al., 2009; Lonati et al., 2010). However, studies have also reported very low PNC, which has been interpreted as

the result of an absence of relevant sources of UFPs such as laser printers (Spinazze et al., 2015).

Parks represent an urban background (UB) site which is not close to any sources. The average PNC value observed in the PK site in London during the daytime was low (7717 ± 4576 cm^{-3}) compared to the PNC value reported by previous studies (Spinazze et al., 2013; Cattaneo et al., 2009). In a study by Aalto et al. (2005), PNC at TI sites were between 2 to 6 times higher than the concentration at the corresponding UB sites in Rome, Barcelona and Stockholm, depending on various factors including distance to the road, traffic volume and sampling height. The average PNC value observed at the TI site in the current study was within the range of previous studies (Spinazze et al., 2015, 2013; Cattaneo et al., 2009; Slezakova et al., 2020), more than 2-times higher compared to the corresponding UB site, supporting the observation from the previous studies. The prime source of pollutants in roadside environments are the vehicular sources (Huang et al., 2021). Apart from direct vehicular emissions, abrasion of vehicle tyres with road and resuspension of road dust also contribute to higher PNC in TI.

The average PM concentration observed in IN, PK, TI and SC sites were less than those reported in previous studies (Wheeler et al., 2000; Harrison et al., 2001; McCreanor et al., 2007; Putaud et al., 2010), even though the traffic levels at SC site were back to normal after the COVID-19 pandemic during the sampling period (Kumar at al., 2022). The improved air quality in London MEs compared with previous studies can also be due to the improved fuel standards, which specify lower sulfur content (Li et al., 2020; Hirota, 2010). We also noted that $PM_{2.5}$, PM_{10} and CO concentrations in all the outdoor MEs were within the WHO global air quality guidelines limits (WHO, 2021). The contrast for PM_{10} concentrations was smaller with a ratio of 1.8 between the street locations and the

312 urban background, adding to the evidence that PM_{10} does not reflect the effect of traffic
313 emissions in the urban MEs (Boogaard et al., 2010).

314 SI Figure S4 shows the CO, CO_2 concentrations and the average temperature and relative
315 humidity (RH) at four MEs during the daytime. SI Figure S5 shows its diurnal variation.
316 CO concentration is higher at the SC site, where the pollutant dispersion is limited (Figure
317 S5a). CO is an indicator of combustion sources which is produced by the incomplete
318 combustion of carbonaceous fuels (Lv et al., 2019), where the highest percentage of CO
319 emissions in developed countries is from the transport sector (Kaur et al., 2005). Higher
320 concentration were observed at IN relative to PK, which is due to the infiltration of CO
321 from the outside, most likely due to the proximity to busy traffic (Chaloulakou and
322 Mavroidis, 2002) but emissions of heating and cooking activities in the kitchen beside
323 the office may have also had an effect (Roden et al., 2009). However, it is less than the
324 WHO limit for indoor CO concentration (WHO, 2010). The variation of indoor CO was
325 smaller than that of outdoor as the rate of concentration reduction is low, leading to
326 increased residence in enclosed space (Chaloulakou et al., 2003). CO_2 concentration was
327 highest at the IN site, which rises abruptly in the office working hours due to the
328 occupancy (Figure S5b). CO_2 concentration is related to ventilation and indoor air quality
329 (IAQ), since lower ventilation rates elevate CO_2 concentration (Persily, 2015). However,
330 the observed CO_2 concentration was less than the recommended CO_2 indoor
331 concentration throughout the day, indicating proper ventilation to the office space. (Du
332 et al., 2020; Mahyuddin and Awbi, 2012). Time plot showing the concentration variation
333 of PM_1, $PM_{2.5}$, PM_{10}, PNC and BC, during the whole monitoring period is also given in
334 SI Figure S6 and S7.

335 **3.2 Diurnal variation of pollutants**

Figure 3 shows the diurnal variation of different pollutants at different MEs. The diurnal variation of PM curves resembles the time-activity pattern of people and road-traffic flow patterns. Different PM fractions (PM_1, $PM_{2.5}$ and PM_{10}) show almost similar trends in the four MEs with higher values for PM_{10}. Figure 3a-c clearly shows that the PM curve at the TI site contains two peaks. PM concentration at TI during daytime was 2 to 3-times higher than the concentration at night. The morning peak reached its maximum between 07:00-9:30 and is associated with the road traffic emissions during morning peak hours. The second peak appeared during the evening rush hours, usually between 16:00-19:00, which can also be explained by the road traffic emissions. It is noted that, in the night-time, PM concentrations (PM_1, $PM_{2.5}$ and PM_{10}) at the TI site were always reduced to become lower than the PK site.

Figure 3a-c shows that PM concentrations were always higher in the morning peak hours than the evening rush hours in both TI and SC, as reported in previous studies (Paton-Walsh et al., 2019). Fine PM fractions (PM_1 and $PM_{2.5}$) at IN did not show much variation with time (Figure 3a-b) as they are difficult to settle, hence always present indoors. But the coarse fraction ($PM_{2.5-10}$) showed an increase in concentration during the office hours while people were present in the office (Figure 3d), most likely due to the resuspension of the coarse particles from movement of people (Persily., 2015). The diurnal profile of PM in PK has an increase in the evening indicating a strong influence of a source with a diurnal pattern of emissions (Harrison and Jones, 2005). The rise in PM concentrations for all the PM fractions in the PK, can also be due to the fugitive PM from the nearby roads due to the vehicular emissions, resuspension, road abrasion, brake and tyre wear etc. (Bigi and Harrison, 2010). It is noted that the increase in PM_1 concentration was high compared to the increase in $PM_{2.5}$ and PM_{10} concentration at the PK site in the evening. The relatively greater increase in PM_1 could have been related to the relative abundance

of fine PM owing to their transport from the nearby roads (Wrobel et al., 2000), and mainly of cooking emissions from the kitchen in the nearby houses (Xiang et al., 2021). It was also observed that the coarse PM ($PM_{2.5-10}$) concentration increased during the daytime (from 07:00 h) at the PK site (Figure 3d). This rise in coarser PM fraction only during the daytime may have also been caused by roof construction work happening in the nearby building during the measurement period.

PNC trend also closely follows the road-traffic flow pattern (Figure 3e), meaning that the meteorological conditions influencing the PNC changed at a smaller rate than road traffic. Different mechanisms are responsible for the production of UFP (which controls the total PNC) and larger particles (which control the mass concentration). So, the relationship between PNC and PMC is not simple, as those mechanisms do not directly co-vary (Harrison and Jones, 2005). Atmospheric residence times for UFP in the boundary layer in cities are relatively short (<1 hour), so their presence in the air can be directly associated with their local emission sources or formation mechanisms (Borsós et al., 2012). Temporal variation of PNC was higher at the street locations. PNC value showed a steep rise in the evening at TI, which consistently increased from 15.00 until 18.30 due to the direct exhaust emissions. The morning and evening peaks were separated by a broad minimum in TI and SC sites, while the concentration remained almost the same in the IN throughout the daytime. The observed TI diurnal variation behaviour for PNC was consistent with the time variations observed in other European cities (Borsós et al., 2012). New particle formation (which usually occurs around midday) also contributes substantially to the UFP (Salma et al., 2011). Since the measurement happened in winter, poor dispersion of local primary emissions in winter is also associated with high PM_{10} and PNC (Harrison and Jones, 2005).

The PNC profile at the PK showed a diurnal variation with a morning rush hour peak typical of an anthropogenic pollutant, which is traffic-related urban pollutants and a PNC rise in the late evening. A number of studies have identified the growth in the number of small particles around midday in urban areas, which can be associated with post noon particle formation with solar radiation (Wehner and Wiedensohler, 2003). The rise in PNC at the PK in the evening could also be due to the influence of fugitive dust emissions from different nearby sources (Harrison and Jones, 2005) as mentioned earlier. Harrison et al. (2004) presented that the airborne particle composition at UK urban background sites is made up from combustion-generated carbonaceous particles, secondary sulfates and nitrates from regional transport, sodium chloride and coarse dusts. BC concentration was higher at IN than PK opposite to that of other pollutants. This is because of the UFP emitted from the printers and the copy machines, which reside inside the room longer.

3.3 Fractional variations of PM at different MEs

There was appreciable day to night differences between fine and coarse particle concentrations, which are indicative of the activities around the MEs. While considering the $PM_1/PM_{2.5}$ ratios, there was a dominance of PM_1 in $PM_{2.5}$ in all the MEs, as the ratio of $PM_1/PM_{2.5}>0.6$ (Figure 4a). Similarly, there was a dominance of $PM_{2.5}$ in PM_{10} in all the MEs. At the TI site, we saw that PM_1 dominance in $PM_{2.5}$ increases after 07:00 in the morning, showing the fine PM fraction coming from the vehicles (Figure 4c). But when we see $PM_{2.5}/PM_{10}$, the amount of $PM_{2.5}$ decreases from 07:00 in the morning, when road traffic is increasing, showing the dominance of coarse fraction ($PM_{2.5-10}$) coming from tyre wear and the dust from non-exhaust emissions from the road. Similar increase in coarser particle concentration was observed in a previous study (Harrison et al., 2001), indicating anthropogenic activities. The results showed that the vehicle induced

409 resuspension provides approximately an equal amount of PM equal to that of exhaust
410 emissions.

411 Similarly, at both IN and PK sites we observed a dominance of fine fraction ($PM_{2.5}$) in
412 the night and of coarse fraction ($PM_{2.5-10}$) during the daytime (Figure 4d). This was due
413 to the resuspension of coarse particles in the floor due to various office activities on the
414 IN site during the daytime. Similarly, at the PK site there is an increase in PM_1 fraction
415 in the evening, while at the TI and SC sites it is reduced during the same period, and the
416 possible reasons are given in Section 3.2. Figure 4c and SI Figure S13 shows the
417 dominance of PM_1 fraction at PK during the night compared to that of SC and TI sites.
418 In PK, the coarse particles during the daytime were made up from non-exhaust emissions
419 generated from the regional transport. In the IN environment, it was observed that the
420 UFP prevailed at nighttime, and the $PM_{1-2.5}$ fraction was increased during the daytime,
421 because of office activities (Figure 4c).

422 Figure 5 shows the pie chart showing the contribution of different PM fractions (PM_1,
423 $PM_{2.5-1}$, $PM_{10-2.5}$) to total PM for IN, TI, PK and SC sites during the daytime. The highest
424 PM_1 fraction was observed in the IN environment as it is difficult to settle, and the air is
425 more stagnant compared to the outdoor MEs. Even though the absolute PM concentration
426 at PK was half to that of the TI site, the fractional contribution pattern of PK followed a
427 similar pattern of TI (SI Figure S8). This shows that the urban background concentrations
428 are made up mainly of the vehicular emissions from the nearby transport (Harrison et al.,
429 2004).

430 **3.4 Exposure assessment**

431 The health risks of individuals depend partly on their daily activities and is also
432 associated with the ambient pollutant concentrations. RDD is the fraction of inhaled

433 particles deposited in the human respiratory tract. We estimated RDD per hour of
434 exposure for PM_1, $PM_{2.5}$ and PM_{10} in different MEs during different physical activities
435 (sitting, walking and running). The ventilation rates of males are usually 23-32% higher
436 than that of females, which gives an equivalent difference in RDD calculations between
437 them. We estimated the RDD for females (31-41 years old) and for children (girls, 3-6
438 years old) and are referring to them in this section (Figure 6). A similar pattern was
439 obtained in males (31-41 years old) and for children (boys, 3-6 years old), which is
440 included in the SI (SI Figure S9).

441 RDD for PM_1 is higher at TI followed by SC and PK, and was least at IN. The estimated
442 RDD variation for PM_1 was 0.28-2.45 μg hr^{-1} for adult females, 0.35-2.99 μg hr^{-1} for adult
443 males and 0.28-1.90 μg hr^{-1} for girl children while performing various physical activities
444 at different MEs (SI, Table S4). PM_1 concentration was observed to be more at IN than
445 PK, while RDD is higher at PK than IN environment, as the deposition fraction depends
446 on the MMD of the particles. Similarly, $PM_{2.5}$ and PM_{10} concentrations were greater at
447 TI than SC, while RDD is higher at SC than TI environment, due to the change in
448 deposition fraction. For the $PM_{2.5}$ size fraction, the RDD variation ranged 0.45-11.22 μg
449 hr^{-1}, 0.55-13.73 μg hr^{-1} and 0.44-8.72 μg hr^{-1} for an adult female, an adult male and a girl
450 child respectively. The female and male RDD for $PM_{2.5}$ was similar to the average person
451 exposure value reported by Lim et al. (2012). For PM_{10}, the observed RDD variation
452 ranged 2.69-37.17 μg hr^{-1}, 3.30-45.46 μg hr^{-1} and 2.64-28.88 μg hr^{-1} for an adult female,
453 an adult male and a girl child respectively during different activities at different MEs (SI
454 Table S4).

455 The RDD for fine particles for walking mode at the TI site (6.63 μg hr^{-1}) was comparable
456 to that reported by Kumar et al. (2018). Likewise, RDD for $PM_{2.5}$ at TI were comparable

to the RDD rates at a similar 4-way TI at Guildford, UK as reported (7 μg hr^{-1}) by Kumar and Goel (2016). However, the estimated RDD for PM_1 was slightly less and RDD for PM_{10} is slightly more, compared to this study. It is noted that the RDD for adult females while walking and running at PK, for PM_1, $PM_{2.5}$ and PM_{10} was 39%, 43% and 53% lower than that at TI or SC. These overall reductions in RDD for all PM fractions between roadsides and parks should be noted while considering the exposure during daily exercises. These findings imply that personal exposures can depend on activity patterns and the microenvironmental concentration. Hence the management of personal exposure should consider potential doses at different MEs during different physical activities for curtailing adverse health effects.

3.5 Micro and nanoscale imaging and chemical analysis

3.5.1 IN, TI and PK sites

IN, TI and PK sites were compared first to provide a baseline for intra-site variability by comparing pollution $PM_{2.5}$ collected using the same MiniVol sampler. At these sites, PM with varied diameters and compositions were observed on the quartz filters by ESEM, with EDXS used to produce elemental maps (Figure 7 a, e, i for IN, TI, PK, respectively). The diameters and spectra of selected particles shown for IN (b-d), TI (f-h) and PK (j-l) indicated agglomeration and co-location of different compounds. The PM in all MEs were composed of Na, Ca, C, O, Si, Cl, Ca and Fe, with Na and Cl co-located together suggesting they are NaCl salt particles arising from either human sweat or sea brine. Fe is a common crustal element but also arises from brake wear (Dall'Osto et al., 2013). Elevated levels of crustal elements (Si, Ca, Fe) can also be produced by diesel engines (Wang et al., 2003), which still form a significant proportion of vehicles in London. Qualitatively, the SEM-EDXS maps showed that the composition and

structure of the particles was similar at all sites, and most probably from traffic-related emissions.

To probe the structure and granularity of the individual PM, at the nm-scale, STEM-EDXS of PM collected at these sites was used. This high-resolution imaging indicated the presence of individual micrometre-sized particles (at all of the IN, TI, PK sites in SI, Figure S10) composed of nanostructures rich in different metals and a composite matrix made up most often of C and O. However, at IN, most particles did not contain these metallic nanostructures: high resolution STEM images and EDX maps of the IN pollution (SI, Figure S10e) showed that they were mostly composed of ultrafine ~20 nm diameter carbon and oxygen-rich particles with graphitic layers that are consistent with those seen in soot reported by Pósfai (2003). This confirms the emission of carbonaceous particles from the printers and copy machines in the office room (Setyawati et al., 2020). At TI and PK, some individual particles had possibly formed larger agglomerates, with the smallest observed particles (<500nm) often composed of metals, for example Fe, Ti, Cr, Al and Mg (SI, Figure S10h, i, o, t).

Interestingly, the STEM-EDX results for $PM_{2.5}$ at the PK and TI sites were made up of hybrid, micrometre-sized particles that contained smaller UFPs, composed of trace metals. This particle structure could potentially break down in the lung, releasing these smaller UFPs that will be more bioreactive due to their higher specific surface area. Prior work has shown that PAHs are commonly associated with fine particles (Miguel et al., 2004), and some types of PAH can adsorb onto PM. Here we identified specific types, such as naphthalene (SI, Table S5), which could be extremely toxic, and carcinogenic to humans, such as those in Group 1, 2A or 2B (IARC, 2010), particularly if they are delivered into the deep lung or even inside lung cells on the surface of a particle. Samples

505 collected from IN, TI and PK sites contain responses from 4 to 7 ring PAH, including
506 benzo(a)pyrene (B[a]P) which is commonly used as a marker for carcinogenic PAHs. In
507 the UK 0.25 ng m^{-3} B[a]P is recommended as an annual average air quality standard
508 (DEFRA, 2007). None of our samples in any of the MEs exceed this limit, however the
509 maximum value of 0.18 ng m^{-3} was found at the IN site. The lower exposure to UV/visible
510 light at IN is likely to mean lower rates of photo-oxidation, which may explain the
511 elevated levels of >4 ring PAHs at IN site.

512 **3.5.2 SC site**

513 At the SC site, PU foams were used to collect and analyse size-fractionated PM
514 using a Harvard impactor, to analyse PM chemistry and morphology across the $PM_{0.1\text{-}2.5}$,
515 $PM_{2.5\text{-}10}$ and $PM_{\geq 10}$ fractions. PM collected at the SC site showed a large variation in
516 morphologies and chemistries and UFPs were observed (Figure 8a-c and Figure S11d).
517 Regardless of the nominal size fraction, in each range large >50 μm agglomerates of
518 particles could be observed as well as individual particles of diameter <400 nm. The most
519 common elements detected in the particles were C, O, Na, Mg, Al, Si, P, S, Cl, K, Ca, Ti,
520 Cr, Mn and Fe (Figure 8d-g) with some variability in the composition of different
521 particles. TEM showed Ti and Fe rich particles of around 400 nm diameter (Figure S11d,
522 e) which are agglomerated into a coarse particle. The composition and structure of the
523 particles was similar to that characterised in the other MEs, and most probably from
524 traffic-related emissions, with the exception of Ca-rich particles, observed in the Ca EDX
525 map, which were only observed at the SC site. Ca is a crustal element present in road dust
526 and building materials; it can arise from road surface abrasion (Saracho et al., 2021). A
527 construction source at the SC compared to the TI is likely to explain the presence of these
528 particles at the SC.

The next step was to perform chemical analysis by ICP-MS of fractionated PM ($PM_{\geq 10}$, $PM_{2.5-10}$ and $PM_{0.1-2.5}$) at SC and PK sites for understanding the source of PM at the PK sites and explaining the diurnal variations in concentrations at these sites (Figures 4c, d). ICP-MS showed that at both locations, fractions were made up of the same elements, but the contribution of metals in the smaller $PM_{0.1-2.5}$ fraction was greater for Na, Al and P at the PK site (SI Figure S12). Fe (1.3 ng m^{-3}) was present at the highest proportion in $PM_{\geq 10}$ at SC site and across all size fractions at an order of magnitude larger concentration than at the PK site (0.06-0.03 ng m^{-3}). Similarly, Mn and Cr were seen in larger concentrations at the SC site. This is consistent with findings of higher total PNC and PM at SC (Figure 2). However, for the fine fraction ($PM_{0.1-2.5}$) this trend was reversed: this may relate to the broad minimum in the $PM_1/PM_{2.5}$ ratio seen in the SC after 18:00h and overnight at the TI, for which the finer sizes PM_1 and $PM_{2.5}$ are lower than that at the PK site overnight (Section 3.3). It is also clear from SI Figure S13 that the relative proportion of PM_1/PM_{10} increases at the PK site after 17.00 h. The reason for relative increase in the PM_1/PM_{10} ratio at the PK overnight is unclear but could arise because fine grained materials transport over a longer distance than the coarse fraction and increase their relative abundance as they move away from the pollution source such as the busy roads nearby (Wrobel et al., 2000), or because of evening activities, such as cooking, in the residential buildings around the park.

To help identify potential sources of the PM collected in each ME and compare the relative abundance of different elements, we subsequently collected SEM-EDXS maps of 100s of particles (n = 121 for IN, n = 300 for PK, n = 260 for TI, and n = 277 for SC sites) at each site and measured the concentration in % and the correlation of the major elements detected in each ME (SI Figure S14). These correlations are discussed in the SI

553 section S5. A similar relative abundance of elements was measured by SEM-EDXS
554 (Figure S14b) at the TI, PK, and IN which implies either similar particle generation
555 activities at these sites or effective atmospheric communication and mixing between
556 sampling locations. If the latter interpretation is correct, then pollution mitigation
557 strategies at source will have a wide geographical impact. A slightly different elemental
558 fingerprint was measured at the SC site compared to the other sites suggesting different
559 local sources of pollution or relative isolation from atmospheric transport.

560 Given that the fine fraction of PM can penetrate the respiratory system and deposit in the
561 lung (Sturm et al., 2016; Kumar et al., 2022c), our data suggest that at the concentrations
562 measured, notably the PM sizes and chemistries characterised here (notably Fe and Cr)
563 could cause toxicity following inhalation, particularly in the TI and SC site (Figure 3)
564 (Bhabra et al., 2009; Charrier and Anastasio, 2015). The presence of transition metals
565 such as Fe and Mn within the fine particles is concerning because of their ability to
566 generate reactive oxygen species (ROS) which can result in inflammatory responses and
567 cellular damage (Valko et al., 2016). ROS in the airways can react to form hydrogen
568 peroxide and hydroxyl radicals which are toxic for the body (Van Klaveren and Nemery,
569 1999). This may result in arrest of protein translation and increased inflammatory
570 mediator production (Cooper and Loxham, 2019) that leads to oxidative stress linked to
571 diseases such as asthma and COPD (Bathri et al., 2017; McGuinness and Sapey, 2017).

572 **4. Summary and conclusions**

573 This study presented the air pollutant concentration data from four different MEs
574 (IN, TI, PK and SC) in London. It provided an overview of the variability of different
575 pollutants among these MEs. The following conclusions are drawn:

- $PM_{2.5}$, PM_{10} and PNC exhibited the following trend: TI>SC>PK>IN. Higher concentrations for PM_1 and BC were observed at IN than PK due to the emissions from printers and the trend changed to TI>SC>IN>PK. The mean $PM_{2.5}$ (PNC) values observed at IN, TI, PK and SC were 3.88±3.06 (5672±2934), 9.47±7.05 (16366±11815), 5.11±2.96 (7717±4576), 8.09±4.57 (10951±6445) µg m^{-3} (# cm^{-3}), respectively. We observed slightly less pollutant concentrations in different MEs in London compared to old studies, which might be due to the improved fuel quality.
- The fine PM concentrations at TI and SC sites were 12%-30% higher during the morning peak hours compared to that in the evening peak hours.
- The observed pollutant concentrations at the IN followed the office time and work pattern. However, the variation in fine PM concentration at IN was smaller than that of outdoor MEs. This variation can be presumably due to the internal sources as well as ingress of outdoor PM. Fractionated PM results at TI show that the vehicle-induced resuspension of coarse particles provides approximately an equal amount of PM equal to that of fine exhaust emissions.
- Fine and ultrafine PM containing soot, trace metals, and metal mixtures from crustal and anthropogenic sources, including Fe, Ti, Cr, Mn, Al and Mg were detected at all sites. A chemical fingerprint of the PM, at the TI and SC sites indicated the presence of transition metals and other elements that are normally found in particles generated by abrasion and resuspension at the roadside as well as crustal and gasoline emissions. A similar relative abundance of different elements was measured in the PK, TI and IN sites, which suggests, more generally, a transport of PM between MEs.
- RDD for PM_1 was highest (2.45±2.27 µg h^{-1}) at TI for females during running, while for $PM_{2.5}$ (11.23±6.34 µg h^{-1}) and PM_{10} (37.17±20.82 µg h^{-1}) were highest at SC. RDD variation between the MEs did not follow the PM concentration trend, as the

deposition fraction depends on MMD. RDD at PK was found to be 39%-53% lower compared with TI and SC during running for all the PM fractions. Therefore, appropriately managed places and routes should be selected for physical activities, to lower the individual personal PM exposures in an urban environment.

The following recommendations are drawn:

- Since higher PM concentrations were observed during the morning peak hours than those during evening rush hours at both the TI and SC sites, and potentially toxic metals including Fe, Ni, Mn, and Cr were measured at these sites, busy roads should be avoided during such peak hours. Policies should target reducing the traffic in these MEs, as well as providing lower-pollution modes of transport.
- Policies to reduce the traffic-related pollution at TI and SC sites could include the following strategies: i) prioritise policies that encourage better pedestrian paths and cycle paths, ii) prioritise measures to encourage a more rapid transition to low and zero tailpipe emission vehicles, iii) including the tightening of fuel efficiency, fuel quality and emission standards, and iv) address non-exhaust emissions, such as raised dust and tyre and wear particles to reduce airborne particles.
- PM was composed of the same potentially toxic metals in the IN site as at the TI site, indicating the transport of PM from road traffic to IN. Therefore, we recommend that building designs should provide windows and other openings of the buildings away from busy roads and traffic zones to prevent the ingress of vehicle exhaust as well as provide ventilation systems which efficiently filter out PM, where possible.

Although the goal of this work was achieved by understanding the typical air pollution characteristics of specific sites, simultaneous monitoring can offer additional opportunities for a direct comparison of concentration among several sites. However, the

626 constraints of multi-site simultaneous measurements can include the unavailability of
627 multiple sets of similar research-grade instruments and the manpower to transport and
628 oversee them in parallel. Our study showed that the exposure concentrations vary with
629 different MEs in urban environments, and pollutant concentration also changes
630 depending on the time of the day. We also quantified the metals and PAHs in aerosol
631 particles to allow risk assessment due to these toxic species. Similar studies are
632 recommended to build a comparable database around various cities and different MEs
633 that can allow the risk assessment and the opportunities to reduce exposure inequalities
634 and design exposure mitigation measures.

635 **5. Acknowledgements**

636 This work has been supported by the EPSRC funded project INHALE (Health
637 assessment across biological length scales for personal pollution exposure and its
638 mitigation; EP/T003189/1). The authors thank the INHALE project team from Imperial
639 College London and the University of Edinburgh for valuable discussions, the INHALE
640 project Manager (Claire Dilliway) for helping with the access from the Data Science
641 Institute (DSI), The invention rooms, Secret gardens and from the Council Borough of
642 Hammersmith and Fulham to carry out our fieldworks. We thank Hammersmith Hospital
643 Authorities of Clement Danes House for providing power supply and personal access,
644 and Darsi Wickham for providing access to Imperial Medical Campus for storage,
645 personal access and facilitation. We thank Sean Burke, Dan Sim, Bogdan and Luqman
646 Jalloh from Imperial college for instrument set-up, access and power supply. Prashant
647 Kumar and Mamatha Tomson also acknowledge the support received by the UGPN's
648 dual PhD Studentship Award (2019-22) by the Universities of Surrey and Wollongong
649 to undertake MT's PhD programme. The authors also thank the GCARE team members
650 (Dr. Arvind Tiwari, Dr. Sarkawt Hama, Dr. Abhijith KV) for their help during the early

discussion and during the campaign, Rosella Arcucci, César Quilodrán Casas and Michal Klosowski from Imperial College London for aiding during field measurements and SEM images collection, Jonathan S. Watson for helping the chemical analysis and Dr. Rebekah Moore and Dr. Alex Griffiths at the London Metallomics Facility, funded by the Wellcome Trust (grant 963 reference 202902/Z/16/Z), for ICP-MS measurements.

5. References

Aalto, P., Hämeri, K., Paatero, P., Kulmala, M., Bellander, T., Berglind, N., Bouso, L., Castano-Vinyals, G., Sunyer, J., Cattani, G., Marconi, A., 2005. Aerosol particle number concentration measurements in five European cities using TSI-3022 condensation particle counter over a three-year period during health effects of air pollution on susceptible subpopulations. J Air & Waste Manag Assoc. 55, 1064-1076.

Abhijith, K.V., Kumar, P., 2021. Evaluation of respiratory deposition doses in the presence of green infrastructure. Air Qual. Atmos. Health. 14, 911-924.

Abhijith, K. V, Kumar, P., 2019. Field investigations for evaluating green infrastructure effects on air quality in open-road conditions. Atmos. Environ. 201, 132–147.

Abhijith, K.V., Kumar, P., Gallagher, J., McNabola, A., Baldauf, R., Pilla, F., Broderick, B., Di Sabatino, S., Pulvirenti, B., 2017. Air pollution abatement performances of green infrastructure in open road and built-up street canyon environments – a review. Atmos. Environ. 162, 71–86.

Air Quality Expert Group. Particulate matter in the UK: summary. 2005. Available at: https://uk-air.defra.gov.uk/assets/documents/reports/aqeg/pm-summary.pdf (accessed: 11 June 2020).

674 Anderson, J.O., Thundiyil, J.G., Stolbach, A., 2012. Clearing the air: a review of the
675 effects of particulate matter air pollution on human health. J Med toxicol. 8, 166-
676 175.
677 Bathri, R., Bose, P., Gujar, V.S., Kumar, L., 2017. The role of ROS in COPD progression
678 and therapeutic strategies. React. Oxyg. Species. 4, 237-250.
679 Berghmans, P., Bleux, N., Panis, L.I., Mishra, V.K., Torfs, R., Van Poppel, M., 2009.
680 Exposure assessment of a cyclist to PM_{10} and ultrafine particles. Sci. Total Environ.
681 407, 1286-1298.
682 Bigi, A., Harrison, R.M., 2010. Analysis of the air pollution climate at a central urban
683 background site. Atmos. Environ. 44, 2004-2012.
684 Birmili, W., Weinhold, K., Rasch, F., Sonntag, A., Sun, J., Merkel, M., Wiedensohler,
685 A., Bastian, S., Schladitz, A., Löschau, G., Cyrys, J., Pitz, M., Gu, J., Kusch, T.,
686 Flentje, H., Quass, U., Kaminski, H., Kuhlbusch, T.A.J., Meinhardt, F., Schwerin,
687 A., Bath, O., Ries, L., Gerwig, H., Wirtz, K., Fiebig, M., 2016. Long-term
688 observations of tropospheric particle number size distributions and equivalent black
689 carbon mass concentrations in the German Ultrafine Aerosol Network (GUAN).
690 Earth Syst. Sci. Data. 8, 355–382.
691 Boogaard, H., Montagne, D.R., Brandenburg, A.P., Meliefste, K., Hoek, G., 2010.
692 Comparison of short-term exposure to particle number, PM_{10} and soot
693 concentrations on three (sub) urban locations. Sci. Total Environ. 408, 4403–4411.
694 Borsós, T., Řimnáčová, D., Ždímal, V., Smolík, J., Wagner, Z., Weidinger, T., Burkart,
695 J., Steiner, G., Reischl, G., Hitzenberger, R., Schwarz, J., Salma, I., 2012.
696 Comparison of particulate number concentrations in three Central European capital
697 cities. Sci. Total Environ. 433, 418–426.

Brzozowski, K., Ryguła, A., Maczyński, A., 2019. The use of low-cost sensors for air quality analysis in road intersections. Transp. Res. Part D: Trans. Environ. 77, 198–211.

Carslaw, D.C., Ropkins, K., 2012. Openair—an R package for air quality data analysis. Environ. Model. Sofw. 27, 52-61.

Cattaneo, A., Garramone, G., Taronna, M., Peruzzo, C., Cavallo, D.M., 2009. Personal exposure to airborne ultrafine particles in the urban area of Milan. J. Phys. Conf. Ser. 151, 012039.

Chaloulakou, A., Mavroidis, I., 2002. Comparison of indoor and outdoor concentrations of CO at a public school. Evaluation of an indoor air quality model. Atmos. Environ. 36, 1769-1781.

Chaloulakou, A., Mavroidis, I., Duci, A., 2003. Indoor and outdoor carbon monoxide concentration relationships at different microenvironments in the Athens area. Chemosphere, 52, 1007-1019.

Chapman, L., Bell, C., Bell, S., 2017. Can the crowdsourcing data paradigm take atmospheric science to a new level? A case study of the urban heat island of London quantified using Netatmo weather stations. Int. J Climatol. 37, 3597-3605.

Cooper, D. M., Loxham, M., 2019. Particulate matter and the airway epithelium: the special case of the underground?. Eur. Respir. Rev. 28, 153.

Dall'Osto, M., Querol, X., Alastuey, A., Minguillon, M. C., Alier, M., Amato, F., Brines, M., Cusack, M., Grimalt, J. O., Karanasiou, A., Moreno, T., Pandolfi, M., Pey, J., Reche, C., Ripoll, A., Tauler, R., Van Drooge, B. L., Viana, M., Harrison, R. M., Gietl, J., Beddows, D., Bloss, W., O'Dowd, C., Ceburnis, D., Martucci, G., Ng, N. L., Worsnop, D., Wenger, J., Mc Gillicuddy, E., Sodeau, J., Healy, R., Lucarelli, F., Nava, S., Jimenez, J. L., Gomez Moreno, F., Artinano, B., Prévôt, A. S. H.,

723 Pfaffenberger, L., Frey, S., Wilsenack, F., Casabona, D., Jiménez-Guerrero, P.,
724 Gross, D., Cots, N., 2013. Presenting SAPUSS: Solving Aerosol Problem by Using
725 Synergistic Strategies in Barcelona, Spain, Atmos. Chem. Phys., 13, 8991–9019.
726 DEFRA, 2018. Clean Air Strategy; Department for Environment Food and Rural Affairs:
727 London, UK. Available at: https://consult.defra.gov.uk/environmental-
728 quality/clean-air-strategy-consultation/user_uploads/clean-air-strategy-2018-
729 consultation.pdf (accessed: 04 April 2022).
730 DEFRA, 2007. The Air Quality Strategy for England, Scotland, Wales and Northern
731 Ireland.
732 Du, B., Tandoc, M.C., Mack, M.L., Siegel, J.A., 2020. Indoor CO_2 concentrations and
733 cognitive function: a critical review. Indoor air, 30, 1067-1082.
734 Fine, P.M., Chakrabarti, B., Krudysz, M., Schauer, J.J., Sioutas, C., 2004. Diurnal
735 variations of individual organic compound constituents of ultrafine and
736 accumulation mode particulate matter in the Los Angeles basin. Environ. Sci.
737 Technol. 38, 1296-1304.
738 Goel, A., Kumar, P., 2014. A review of fundamental drivers governing the emissions,
739 dispersion and exposure to vehicle-emitted nanoparticles at signalised traffic
740 intersections. Atmos. Environ. 97, 316–331.
741 Gomes, J.F.P., Bordado, J.C.M., Albuquerque, P.C.S., 2012. On the assessment of
742 exposure to airborne ultrafine particles in urban environments. J. Toxicol. Environ.
743 Heal. - Part A Curr. Issues 75, 1316–1329.
744 Hagler, G.S.W., Yelverton, T.L.B., Vedantham, R., Hansen, A.D.A., Turner, J.R., others,
745 2011. Post-processing method to reduce noise while preserving high time
746 resolution in aethalometer real-time black carbon data. Aerosol Air Qual. Res. 11,
747 539–546.

748 Hama, S.M.L., Cordell, R.L., Monks, P.S., 2017. Quantifying Primary and Secondary
749 Source Contributions to Ultrafine Particles in the UK Urban Background. Atmos.
750 Environ. 166, 62-78.
751 Harrison, R.M., Jones, A.M., 2005. Multisite study of particle number concentrations in
752 urban air. Environ. Sci. Technol. 39, 6063–6070.
753 Harrison, R.M., Jones, A.M., Lawrence, R.G., 2004. Major component composition of
754 PM_{10} and $PM_{2.5}$ from roadside and urban background sites. Atmos. Environ. 38,
755 4531–4538.
756 Harrison, R.M., Yin, J., Mark, D., Stedman, J., Appleby, R.S., Booker, J., Moorcroft, S.,
757 2001. Studies of the coarse particle (2.5-10 μm) component in UK urban
758 atmospheres. Atmos. Environ. 35, 3667–3679.
759 Heinzerling, A., Hsu, J., Yip, F., 2016. Respiratory health effects of ultrafine particles in
760 children: A literature review. Water Air Soil Pollut. 227, 1-14.
761 Hinds, W.C., 1999. Aerosol Technology: Properties, Behavior, and Measurement of
762 Airborne Particles. second ed. Ed. John Wiley & Sons, New York.
763 Hirota, K., 2010. Comparative studies on vehicle related policies for air pollution
764 reduction in ten Asian countries. Sustainability, 2, 145-162.
765 Huang, Y., Lei, C., Liu, C.H., Perez, P., Forehead, H., Kong, S. and Zhou, J.L., 2021. A
766 review of strategies for mitigating roadside air pollution in urban street canyons.
767 Environ. Pollut. 280, 116971.
768 IARC Working Group on the Evaluation of Carcinogenic Risks to Humans, 2010. Some
769 non-heterocyclic polycyclic aromatic hydrocarbons and some related exposures.
770 IARC Monogr. Eval. Carcinog. Risks Hum. 92, 1-853.

771 ICRP, 1994. Human respiratory tract model for radiological protection: a report of a task
772 group of the International Commission on Radiological Protection. ICRP
773 Publication, 66 0080411541, 1-482.
774 Jones, N.C., Thornton, C.A., Mark, D., Harrison, R.M., 2000. Indoor/outdoor
775 relationships of particulate matter in domestic homes with roadside, urban and rural
776 locations. Atmos. Environ. 34, 2603–2612.
777 Kaur, S., Nieuwenhuijsen, M., Colvile, R., 2005. Personal exposure of street canyon
778 intersection users to $PM_{2.5}$, ultrafine particle counts and carbon monoxide in Central
779 London, UK. Atmos. Environ. 39, 3629-3641.
780 Kolokotroni, M., Zhang, Y., Watkins, R., 2007. The London Heat Island and building
781 cooling design. J. Sol. Energy. 81, 102-110.
782 Kumar, P., Goe,l A., 2016. Concentration dynamics of coarse and fine particulate matter
783 at and around signalised traffic intersections. Environ. Sci. Process Impacts.
784 18,1220–1235.
785 Kumar, P., Gurjar, B.R., Nagpure, A. S., Harrison, R.M., 2011a. Preliminary Estimates
786 of Nanoparticle Number Emissions from Road Vehicles in Megacity Delhi and
787 Associated Health Impacts. Environ. Sci. Technol. 45, 5514–5521.
788 Kumar, P., Hama, S., Abbass, R.A., Nogueira, T., Brand, V.S., Wu, H.W., Abulude, F.O.,
789 Adelodun, A.A., Anand, P., de Fatima Andrade, M., Apondo, W., 2022a. In-kitchen
790 aerosol exposure in twelve cities across the globe. Environ. Int. 162, 107155.
791 Kumar, P., Kalaiarasan, G., Porter, A.E., Pinna, A., Kłosowski, M.M., Demokritou, P.,
792 Chung, K.F., Pain, C., Arvind, D.K., Arcucci, R., Adcock, I.M., 2021. An overview
793 of methods of fine and ultrafine particle collection for physicochemical
794 characterisation and toxicity assessments. Sci. Total Environ. 756.

795 Kumar, P., Rivas, I., Sachdeva, L., 2017. Exposure of in-pram babies to airborne particles
796 during morning drop-in and afternoon pick-up of school children. Environ. Pollut.
797 224, 407–420.
798 Kumar, P., Rivas, I., Singh, A. P., Ganesh, V. J., Ananya, M., Frey, H. C., 2018.
799 Dynamics of coarse and fine particle exposure in transport microenvironments.
800 Clim. Atmos. Sci. 11, 1–12.
801 Kumar, P., Zavala-Reyes, J.C., Tomson, M., Kalaiarasan, G., 2022b. Understanding the
802 effects of roadside hedges on the horizontal and vertical distributions of air
803 pollutants in street canyons. Environ. Int. 158, 106883.
804 Kumar, P., Zavala-Reyes, J.C., Kalaiarasan, G., Abubakar-Waziri, H., Young, G.,
805 Mudway, I., Dilliway, C., Lakhdar, R., Mumby, S., Klosowski, M. K., Pain, C.,
806 Adcock, I. M., Watson, J. S., Sephton, M. A., Chung, K.F., Porter, A.E, 2022c.
807 Characteristics of Fine and Ultrafine Aerosols in the London Underground. Under
808 review.
809 Li, P., Lu, Y., Wang, J., 2020. The effects of fuel standards on air pollution: Evidence
810 from China. J. Dev. Econ. 146, 102488.
811 Lim, S., Kim, J., Kim, T., Lee, K., Yang, W., Jun, S., Yu, S., 2012. Personal exposures
812 to $PM_{2.5}$ and their relationships with microenvironmental concentrations. Atmos.
813 Environ. 47, 407–412.
814 Lonati, G., Ozgen, S., Luraghi, I., Giugliano, M., 2010. Particle number concentration at
815 urban microenvironments, in: Chemical Engineering Transactions. Ital. Assoc.
816 Chem. Eng - AIDIC. 137–142.
817 Luengo-Oroz, J., Reis, S., 2019. Assessment of cyclists' exposure to ultrafine particles
818 along alternative commuting routes in Edinburgh. Atmos. Pollut. Res. 10, 1148-
819 1158.

820 Lv, W., Hu, Y., Li, E., Liu, H., Pan, H., Ji, S., Hayat, T., Alsaedi, A., Ahmad, B., 2019.
821 Evaluation of vehicle emission in Yunnan province from 2003 to 2015. J. Clean.
822 Prod. 207, 814-825.
823 Mahyuddin, N., Awbi, H., 2012. A review of CO_2 measurement procedures in ventilation
824 research. Int. J. Vent. 10, 353-370.
825 Mazaheri, M., Clifford, S., Yeganeh, B., Viana, M., Rizza, V., Flament, R., Buonanno,
826 G., Morawska, L., 2018. Investigations into factors affecting personal exposure to
827 particles in urban microenvironments using low-cost sensors. Environ. Int. 120,
828 496-504.
829 McCreanor, J., Cullinan, P., Nieuwenhuijsen, M.J., Stewart-Evans, J., Malliarou, E.,
830 Jarup, L., Harrington, R., Svartengren, M., Han, I.K., Ohman-Strickland, P.,
831 Chung, K.F., Zhang, J. 2007. Respiratory effects of exposure to diesel traffic in
832 persons with asthma. N. Engl. J. Med. 357, 2348–2358.
833 McGuinness, A.J.A., Sapey, E., 2017. Oxidative stress in COPD: sources, markers, and
834 potential mechanisms. J. Clin. Med. 6, 21.
835 Miao, X., Li, W., Niu, B., Li, J., Sun, J., Qin, M., Zhou, Z., 2019. Mitochondrial
836 dysfunction in endothelial cells induced by airborne fine particulate matter (<2.5
837 μm). J Appl Toxicol. 39, 1424– 1432.
838 Miguel, A.H., Eiguren-Fernandez, A., Jaques, P.A., Froines, J.R., Grant, B.L., Mayo,
839 P.R., Sioutas, C., 2004. Seasonal variation of the particle size distribution of
840 polycyclic aromatic hydrocarbons and of major aerosol species in Claremont,
841 California. Atmos. Environ. 38, 3241–3251.
842 Miller, S.L., Facciola, N.A., Toohey, D., Zhai, J., 2017. Ultrafine and fine particulate
843 matter inside and outside of mechanically ventilated buildings. Int. J. Environ. Res.
844 Public Health, 14, 128.

Mohammadyan, M., Keyvani, S., Bahrami, A., Yetilmezsoy, K., Heibati, B., Godri Pollitt, K.J., 2019. Assessment of indoor air pollution exposure in urban hospital microenvironments. Air Qual. Atmos. Health, 12, 151-159.

Paton-Walsh, C., Rayner, P., Simmons, J., Fiddes, S.L., Schofield, R., Bridgman, H., Beaupark, S., Broome, R., Chambers, S.D., Chang, L.T.C., Cope, M., 2019. A clean air plan for Sydney: An overview of the special issue on air quality in New South Wales. Atmosphere, 10, 774.

Persily, A.K., 2015. Indoor carbon dioxide concentrations in ventilation and indoor air quality standards. 36th AIVC Conference Effective Ventilation in High Performance Buildings, Madrid, Spain, 810-819.

Piotrowicz, A., Polednik, B. 2019. Exposure to aerosol particles on an urban road. J. Ecol. Eng. 20, 27–34.

Pósfai, M., Simonics, R., Li, J., Hobbs, P. V., Buseck, P. R., 2003. Individual aerosol particles from biomass burning in southern Africa: 1. Compositions and size distributions of carbonaceous particles. J. Geophys. Res. 108, 8483.

Puett, R.C., Hart, J.E., Yanosky, J.D., Paciorek, C., Schwartz, J., Suh, H., Speizer, F.E., Laden, F., 2009. Chronic fine and coarse particulate exposure, mortality, and coronary heart disease in the Nurses' Health Study. Environ. Health Perspect. 117, 1697–1701.

Putaud, J.-P., Van Dingenen, R., Alastuey, A., Bauer, H., Birmili, W., Cyrys, J., Flentje, H., Fuzzi, S., Gehrig, R., Hansson, H.C., Harrison, R.M., Herrmann, H., Hitzenberger, R., Hüglin, C., Jones, A.M., Kasper-Giebl, A., Kiss, G., Kousa, A., Kuhlbusch, T.A.J., Löschau, G., Maenhaut, W., Molnar, A., Moreno, T., Pekkanen, J., Perrino, C., Pitz, M., Puxbaum, H., Querol, X., Rodriguez, S., Salma, I., Schwarz, J., Smolik, J., Schneider, J., Spindler, G., ten Brink, H., Tursic, J., Viana,

M., Wiedensohler, A., Raes, F., 2010. A European aerosol phenomenology – 3: Physical and chemical characteristics of particulate matter from 60 rural, urban, and kerbside sites across Europe. Atmos. Environ. 44, 1308 -1320.

Qvarfordt, M., Anderson, M., Sanchez-Crespo, A., Diakopoulou, M., Svartengren, M., 2022. Pulmonary translocation of ultrafine carbon particles in COPD and IPF patients. Inhal. Toxicol. 34,14-23.

Rivas, I., Kumar, P., Hagen-Zanker, A., de Fatima Andrade, M., Slovic, A.D., Pritchard, J.P., Geurs, K.T., 2017a. Determinants of black carbon, particle mass and number concentrations in London transport microenvironments. Atmos. Environ. 161, 247–262.

Rivas, I., Kumar, P., Hagen-Zanker, A., 2017b. Exposure to air pollutants during commuting in London: are there inequalities among different socio-economic groups? Environ. Int. 101, 143–157.

Roden, C.A., Bond, T.C., Conway, S., Pinel, A.B.O., MacCarty, N., Still, D., 2009. Laboratory and field investigations of particulate and carbon monoxide emissions from traditional and improved cookstoves. Atmos. Environ. 43, 1170-1181.

Sahu, V., Gurjar, B.R., 2020. Spatial and seasonal variation of air quality in different microenvironments of a technical university in India. Build. Environ. 185, 107310.

Salma, I., Borsós, T., Weidinger, T., Aalto, P., Hussein, T., Maso, M.D., Kulmala, M., 2011. Production, growth and properties of ultrafine atmospheric aerosol particles in an urban environment. Atmos. Chem. Phys. 11, 1339-1353.

Samet, J.M., Chen, H., Pennington, E.R., Bromberg, P.A., 2020. Non-redox cycling mechanisms of oxidative stress induced by PM metals. Free Radic. Biol. Med. 151, 26-37.

894 Saracho, A.C., Lucherini, L., Hirsch, M., Peter, H.M., Terzis, D., Amstad, E., Laloui, L.,
895 2021. Controlling the calcium carbonate microstructure of engineered living
896 building materials. J. Mater. Chem. A. 9, 24438-24451.
897 Schneider, C.A., Rasband, W.S., Eliceiri, K.W., 2012. NIH Image to ImageJ: 25 years of
898 image analysis. Nat. Methods. 9, 671-675.
899 Setyawati, M.I., Singh, D., Krishnan, S.P., Huang, X., Wang, M., Jia, S., Goh, B.H.R.,
900 Ho, C.G., Yusoff, R., Kathawala, M.H., Poh, T.Y., 2020. Occupational inhalation
901 exposures to nanoparticles at six Singapore printing centers. Environ. Sci. Technol.
902 54, 2389-2400.
903 Sharma, A., Kumar, P., 2020. Quantification of air pollution exposure to in-pram babies
904 and mitigation strategies. Environ. Int. 139, 105671.
905 Shrestha, P.M., Humphrey, J.L., Carlton, E.J., Adgate, J.L., Barton, K.E., Root, E.D.,
906 Miller, S.L., 2019. Impact of outdoor air pollution on indoor air quality in low-
907 income homes during wildfire seasons. Int. J. Environ. Res. Public Health, 16,
908 3535.
909 Slezakova, K., Pereira, M.C., Morais, S., 2020. Ultrafine particles: Levels in ambient air
910 during outdoor sport activities. Environ. Pollut. 258, 113648.
911 Spinazzè, A., Cattaneo, A., Garramone, G., Cavallo, D.M., 2013. Temporal variation of
912 size-fractionated particulate matter and carbon monoxide in selected
913 microenvironments of the Milan urban area. J. Occup. Environ. Hyg. 10, 652–662.
914 Spinazzè, A., Cattaneo, A., Scocca, D.R., Bonzini, M., Cavallo, D.M., 2015. Multi-metric
915 measurement of personal exposure to ultrafine particles in selected urban
916 microenvironments. Atmos. Environ. 110, 8–17.
917 Sturm, R., 2016. Total deposition of ultrafine particles in the lungs of healthy men and
918 women: experimental and theoretical results. Ann. Transl. Med. 4, 234.

Thorpe, A., Harrison, R.M., 2008. Sources and properties of non-exhaust particulate matter from road traffic: A review. Sci. Total Environ. 400, 270–282.

Tomson, M., Kumar, P., Barwise, Y., Perez, P., Forehead, H., French, K., Morawska, L., Watts, J.F., 2021. Green infrastructure for air quality improvement in street canyons. Environ. Int. 146, 106288.

US-EPA, 2009. Metabolically derived human ventilation rates: a revised approach based upon oxygen consumption rates (Washington, DC).

Usmani, O.S., Biddiscombe, M.F., Yang, S., Meah, S., Oballa, E., Simpson, J.K., Fahy, W.A., Marshall, R.P., Lukey ,P.T., Maher, T.M., 2018. The topical study of inhaled drug (salbutamol) delivery in idiopathic pulmonary fibrosis. Respir. Res. 19, 25.

Valko, M., Jomova, K., Rhodes, C.J., Kuča, K., Musílek, K., 2016. Redox-and non-redox-metal-induced formation of free radicals and their role in human disease. Arch. Toxicol. 90, 1-37.

Van Klaveren, R.J., Nemery, B., 1999. Role of reactive oxygen species in occupational and environmental obstructive pulmonary diseases. Curr. Opin. Pulm. Med. 5, 118–118.

Voordeckers, D., Meysman, F. J. R., Billen, P., Tytgat, T., Van Acker, M., 2021. The impact of street canyon morphology and traffic volume on NO2 values in the street canyons of Antwerp. Build. Environ. 197, 107825.

Wang, Y. F., Huang, K. L., Li, C. T., Mi, H. H., Luo, J. H., Tsai, P. J., 2003. Emissions of fuel metals content from a diesel vehicle engine. Atmos. Environ. 37, 4637-4643.

Wehner, B., Wiedensohler, A., 2003. Long term measurements of submicrometer urban aerosols: statistical analysis for correlations with meteorological conditions and trace gases. Atmos. Chem. Phys. 3, 867-879.

943 Wheeler, A.J., Williams, I., Beaumont, R.A., Hamilton, R.S., 2000. Characterisation of
944 particulate matter sampled during a study of children's personal exposure to
945 airborne particulate matter in a UK urban environment. Environ. Monit. Assess. 65,
946 69-77.
947 World Health Organization, 2010. WHO guidelines for indoor air quality: selected
948 pollutants. World Health Organization. Regional Office for Europe.
949 World Health Organization, 2018. Available at: https://www.who.int/news-room/fact-
950 sheets/detail/ambient-(outdoor)-air-quality-and-health (accessed: 18 July 2020).
951 World Health Organization, 2021. WHO Global Air Quality Guidelines: Particulate
952 Matter ($PM_{2.5}$ and PM_{10}), Ozone, Nitrogen Dioxide, Sulfur Dioxide and Carbon
953 Monoxide. Available at: https://apps.who.int/iris/handle/10665/345329 (accessed:
954 12.07.2022).
955 Wrobel, A., Rokita, E., Maenhaut, W., 2000. Transport of traffic-related aerosols in urban
956 areas. Sci. Total Environ. 257, 199-211.
957 Xiang, J., Hao, J., Austin, E., Shirai, J., Seto, E., 2021. Characterization of cooking-
958 related ultrafine particles in a US residence and impacts of various intervention
959 strategies. Sci. Total Environ., 798, 149236.

960 Yan, C., Zheng, M., Yang, Q., Zhang, Q., Qiu, X., Zhang, Y., Fu, H., Li, X., Zhu, T.,
961 Zhu, Y., 2015. Commuter exposure to particulate matter and particle-bound PAHs
962 in three transportation modes in Beijing, China. Environ. Pollut. 204, 199–206.

963 Yin, J., Harrison, R.M., 2008. Pragmatic mass closure study for $PM_{1.0}$, $PM_{2.5}$ and PM_{10}
964 at roadside, urban background and rural sites. Atmos. Environ. 42, 980–988.

965 **List of Tables**

966 **Table 1.** Summary of relevant past studies assessing pollutant concentrations in various MEs.

Study type	Study details	City (Country)	Observed MEs	Pollutants measured	Instruments used	Reference
Assessment of indoor air quality in ten different indoor microenvironments	Indoor activities, ventilation and occupancy, were responsible for seasonal and spatial variability among indoor MEs.	Roorkee (India)	Indoor (lecture hall, office, laboratory etc.)	$PM_{2.5}$, PM_{10} and TVOC	GRIMM, TG-503L	Sahu and Gurjar (2020)
Determination of pollutant concentration in two hospitals and outdoors	-Indoor PM_1 and $PM_{2.5}$ concentrations were positively associated with outdoor concentrations, but no relationship was observed with PM_{10}.	Kashan (Iran)	Indoor (hospital), Outdoor	PM_1, $PM_{2.5}$ and PM_{10}	GRIMM	Mohammadyan et al. (2019)
Assessment of personal $PM_{2.5}$ exposures	- Highest personal $PM_{2.5}$ exposure was	Brisbane (Australia)	Indoor (home), Transport MEs	$PM_{2.5}$	Low-cost sensors (Airbeam personal air	Mazaheri et al. (2018)

indoors, outdoors and when commuting	observed at home.				quality and environmental monitor)	
Measurement of personal exposure to UFPs in different urban MEs and modes of transportation	- Concentration variation depends on sources of urban pollutants, proximity to source and time of the day	Como (Italy)	Indoor (office), Traffic intersection	PNC	Diffusion size classifier (DSC) (10nm-700nm), Condensation particle counter (P-TRAK)	Spinazze et al. (2015)
Study on temporal variation of concentration of size-fractionated PM and CO in different MEs	- Atmospheric concentration measurements of UFPs, PM and CO were divided on MEs, seasons, days and time. - Concentration pattern related to sources of urban pollutants (traffic), proximity to source and time of the day	Milan (Italy)	Park, indoor (office), multi-road intersection, metro, walk, car, bus	UFPs, PM and CO	Optical particle counter (OPC), CPC (P-TRAK) and CO analyzer	Spinazze et al. (2013)
Determination of $PM_{2.5}$	- Impact of activity pattern	Seoul (Korea)	Residential indoor,	$PM_{2.5}$	Photometric aerosol	Lim et al. (2012)

exposure in different MEs	and the contribution of each ME to personal $PM_{2.5}$ exposure		non-residential indoor (office, restaurant, bar etc), transportation, outdoor		monitor (SidePak TSI model AM510)	
Comparison of exposure to PNC, PM_{10} and soot concentrations	- Simultaneous measurement at three sites - PNC and soot concentration at street was 3 times of background locations - Mean PNC was poorly correlated with PM_{10} and soot - High PNC temporal variation at street; and less variation at background locations	Utrecht (Netherlands)	Busy street, urban and a suburban background location	PNC, PM_{10}	Harvard impactor, Condensation particle counter (CPC)	Boogaard et al. (2010)
Determination of PNC in different indoor MEs	- Higher concentration in kitchen, which varies with cooking activity	Milan (Italy)	Residential house, office, printer room,	PNC	P-TRAK	Lonati et al. (2010)

and transport MEs	- According to time-weighted exposure scenario, daily average exposure is 16000 particles cm^{-3} for people in Milan		cafe, church, hairdresser, supermarket, pedestrian route, car, subway, train			
Measurement of personal exposure to UFPs in different urban MEs and modes of transportation	- Highest exposure near motorised traffic - Lowest exposure at parks and in office	Milan (Italy)	Park, indoor (office), metro, walk, car, bus	PNC	Condensation particle counters (P-TRAK)	Cattaneo et al. (2009)
Comparison of PM_1, $P_{2.5}$ and PM_{10} at an urban roadside, urban background and rural location	- PM concentration: urban roadside > urban background > rural background; except for PM_1	Birmingham (UK)	Urban roadside, park (urban background) and a rural location	PM_1, $PM_{2.5}$ and PM_{10}	Partisol-Plus sequential air samplers (Model 2025)	Yin and Harrison (2008)

Evaluation of major chemical component composition of urban background PM in UK and determination of roadside increment in $PM_{2.5}$ and PM_{10}	- Major chemical components are: sulfate, nitrate, chloride, organic carbon, elemental carbon, iron and calcium. - Roadside particle increment consists mainly of elemental carbon, organic compounds and iron-rich dusts.	3 pairs in London and 1 pair in Birmingham (UK)	Roadside, urban background location (pedestrian area, garden, park, quiet suburban road)	PM_{10}, $PM_{2.5}$	Dichotomous Partisol samplers	Harrison et al. (2004)
Study on coarse fraction of PM and insights into its sources in the UK	- Considered five different sites. - Noted a remarkable weekday-to-weekend and day-to-night differences between coarse particle concentration at the urban sites, representing anthropogenic activities (vehicle	Birmingham, London (UK)	Urban street canyon, urban background (park)	PM_{10}, $PM_{2.5}$, NO_x	TEOM instruments	Harrison et al. (2001)

	induced resuspension).					

967

968 **Table 2.** Description of number of days of field measurements in different MEs.

Type of ME	Campaign (start – end)	Total days	Remarks / Breaks in monitoring
IN	25.11.2019 - 24.01.2020	43	19.12.2019 - 07.01.2020; Christmas holidays
TI	28.01.2020 - 21.02.2020	17	09.02.2020; Storm Ciara 15.02.2020 - 16.02.2020; Storm Dennis
PK	24.02.2020 - 19.03.2020	25	Continuous monitoring
SC	06.08.2020 - 22.09.2020	36	13.08.2020 - 14.08.2020; Rain 18.08.2020; Rain 21.08.2020; Wind alert

969

970 **Table 3.** Descriptive statistics showing the data availability, mean, standard deviation (SD) and
971 median of pollutant concentration on each of the MEs during daytime. *n* = number of 60
972 seconds averaged data points.

		IN	**TI**	**PK**	**SC**
PM	*n*	20815	8005	12586	6650
PM_1 (µg m^{-3})	Mean	3.19	6.19	3.17	4.94
	SD	2.95	5.76	2.46	3.65
	Median	2.1	3.6	2.5	4.0

$PM_{2.5}$ (µg m^{-3})	Mean	3.88	9.47	5.11	8.09
	SD	3.06	7.05	2.96	4.57
	Median	2.8	6.7	4.6	6.9
PM_{10} (µg m^{-3})	Mean	5.74	14.56	7.97	15.17
	SD	4.04	11.88	4.51	8.5
	Median	4.6	10.5	7.2	13.3
$PM_{2.5-10}$ (µg m^{-3})	Mean	1.86	5.1	2.85	7.08
	SD	2.36	5.8	2.73	5.48
	Median	1.1	3.4	2.2	6.00
$PM_1/PM_{2.5}$	Mean	0.77	0.62	0.60	0.60
	SD	0.41	0.15	0.16	0.16
	Median	0.77	0.61	0.58	0.64
$PM_{2.5}/PM_{10}$	Mean	0.72	0.71	0.67	0.56
	SD	0.26	0.15	0.18	0.13
	Median	0.76	0.71	0.67	0.56
PNC (# cm^{-3})	n	9867	6128	6676	4340
	Mean	5672	16366	7717	10951
	SD	2934	11815	4576	6445
	Median	4844	12841	6312	9202
BC (ng m^{-3})	n	20540	5825	7110	7698
	Mean	771.4	1912.7	521.4	1387.4
	SD	811.3	1649.9	355.26	1532

	Median	484	1334	424	1000
CO_2 (ppm)	n	20509	6120	8169	1738
	Mean	583.12	416.2	373.62	367.96
	SD	101.21	36.79	11.46	18.07
	Median	596	407	372	364
CO (ppm)	Mean	0.9	0.25	0.02	1.58
	SD	2.79	0.52	0.08	1.22
	Median	0	0	0	1.2

973

974 **List of Figures**

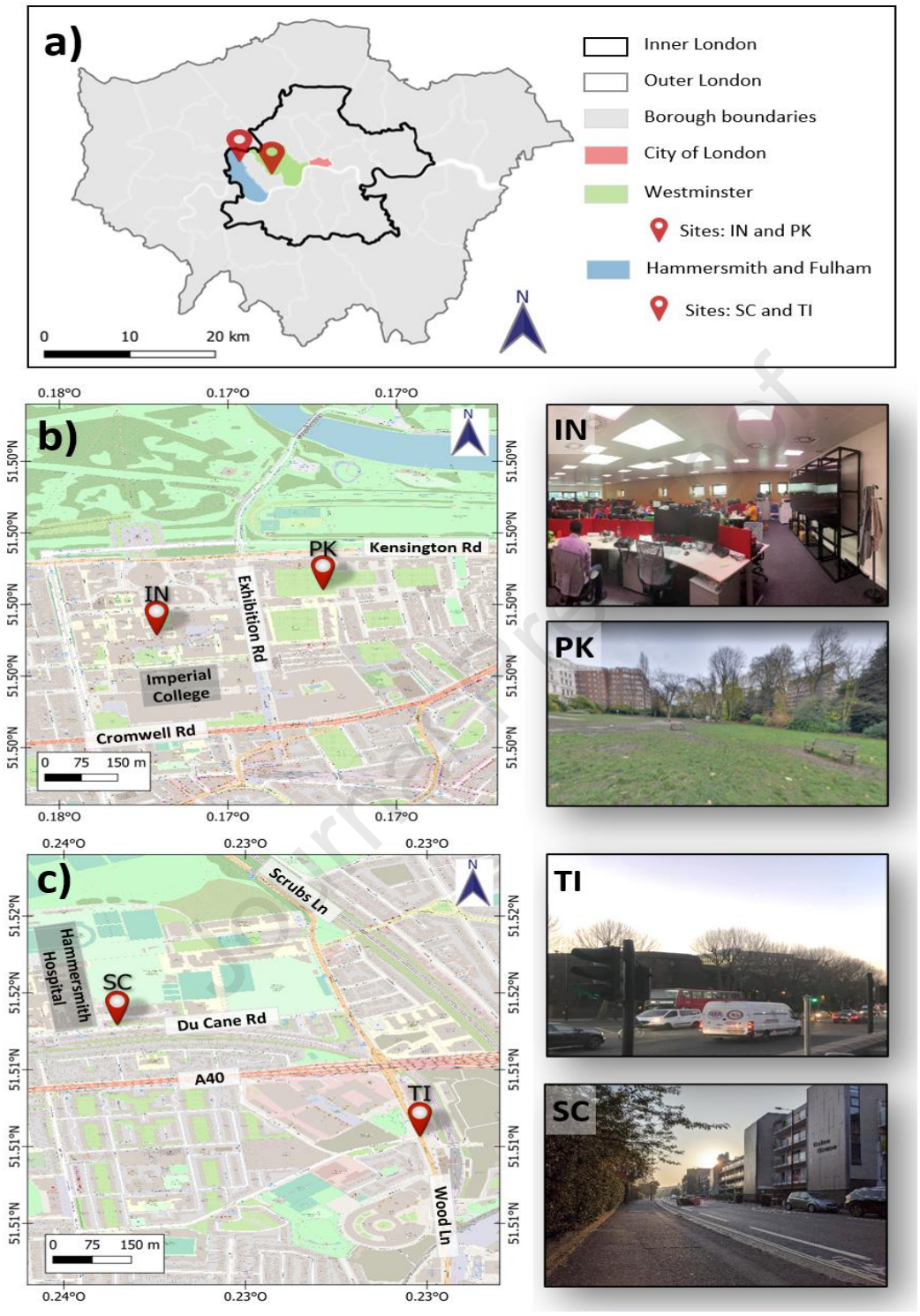

975

976 **Figure 1.** (a) Map showing the location of pollutant measurement sites in two London boroughs
977 (Westminster, and Hammersmith and Fulham). (b) Westminster sites: Indoor (IN) and park
978 (PK); (c) Hammersmith and Fulham sites: Traffic Intersection (TI) and Street Canyon (SC).

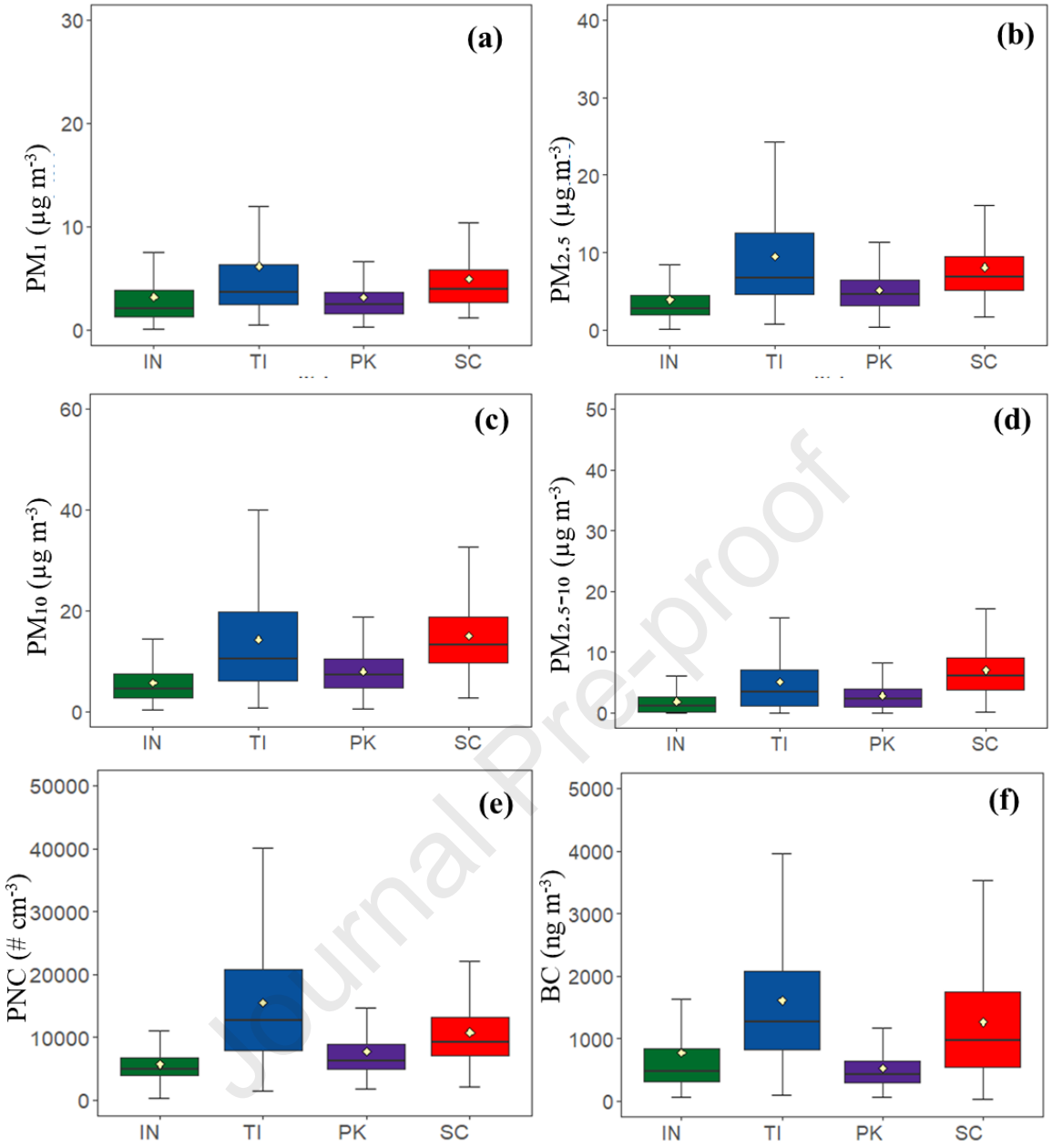

979

980 **Figure 2.** Boxplots of average pollutant concentration of (a) PM_1, (b) $PM_{2.5}$, (c) PM_{10}, (d)
981 $PM_{2.5-10}$, (e) PNC, (f) BC measured at IN, TI, PK and SC sites for the daytime (07:00-19:00).
982 Diamond symbols refer to arithmetic mean concentrations while the median values are shown
983 by horizontal lines within the bars.

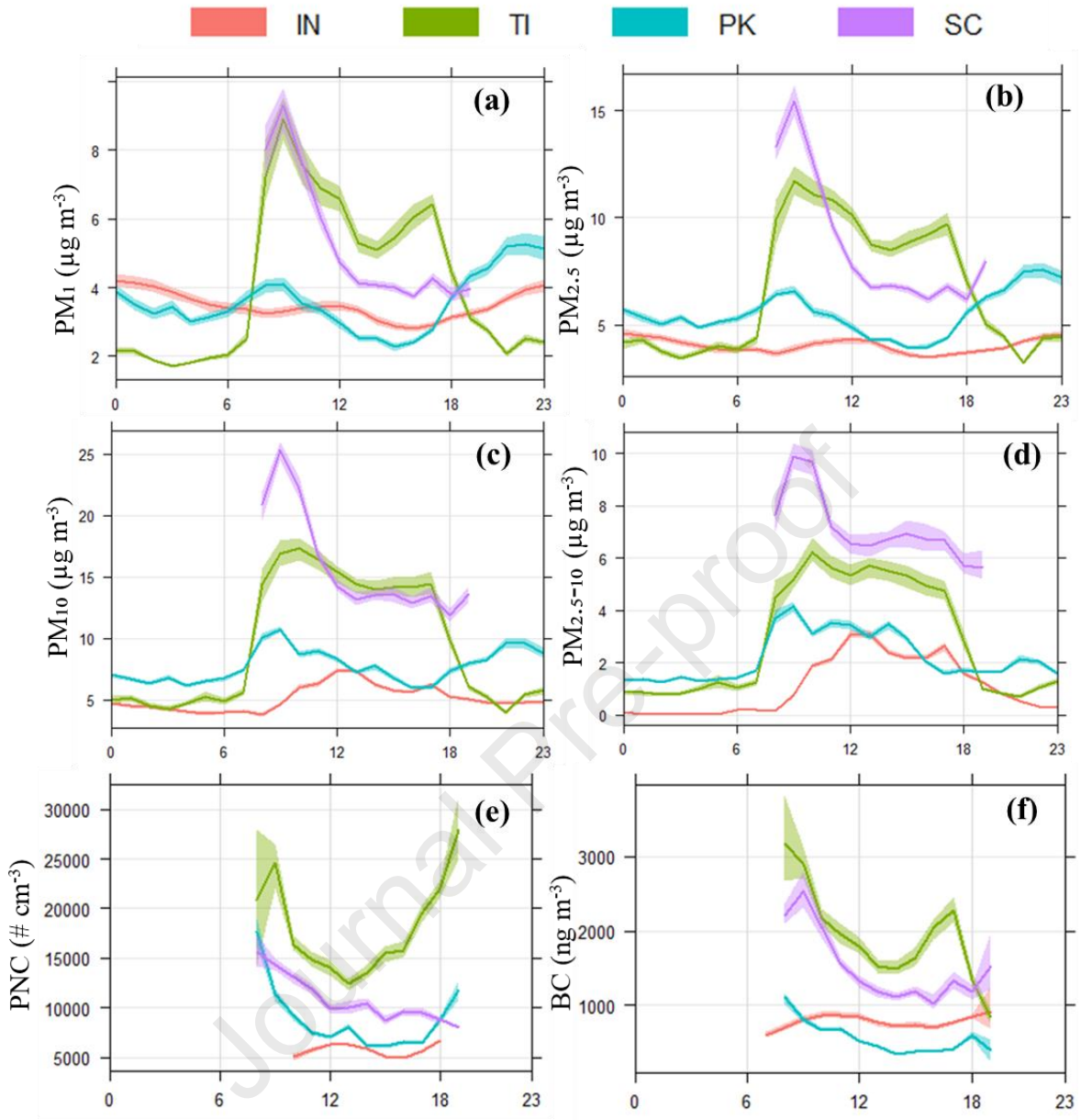

984

985 **Figure 3.** Diurnal variation of pollutant concentration of (a) PM_1, (b) $PM_{2.5}$, (c) PM_{10}, (d)
986 $PM_{2.5-10}$, (e) PNC, (f) BC measured at IN, TI, PK and SC sites. The shaded area indicates 95%
987 confidence intervals.

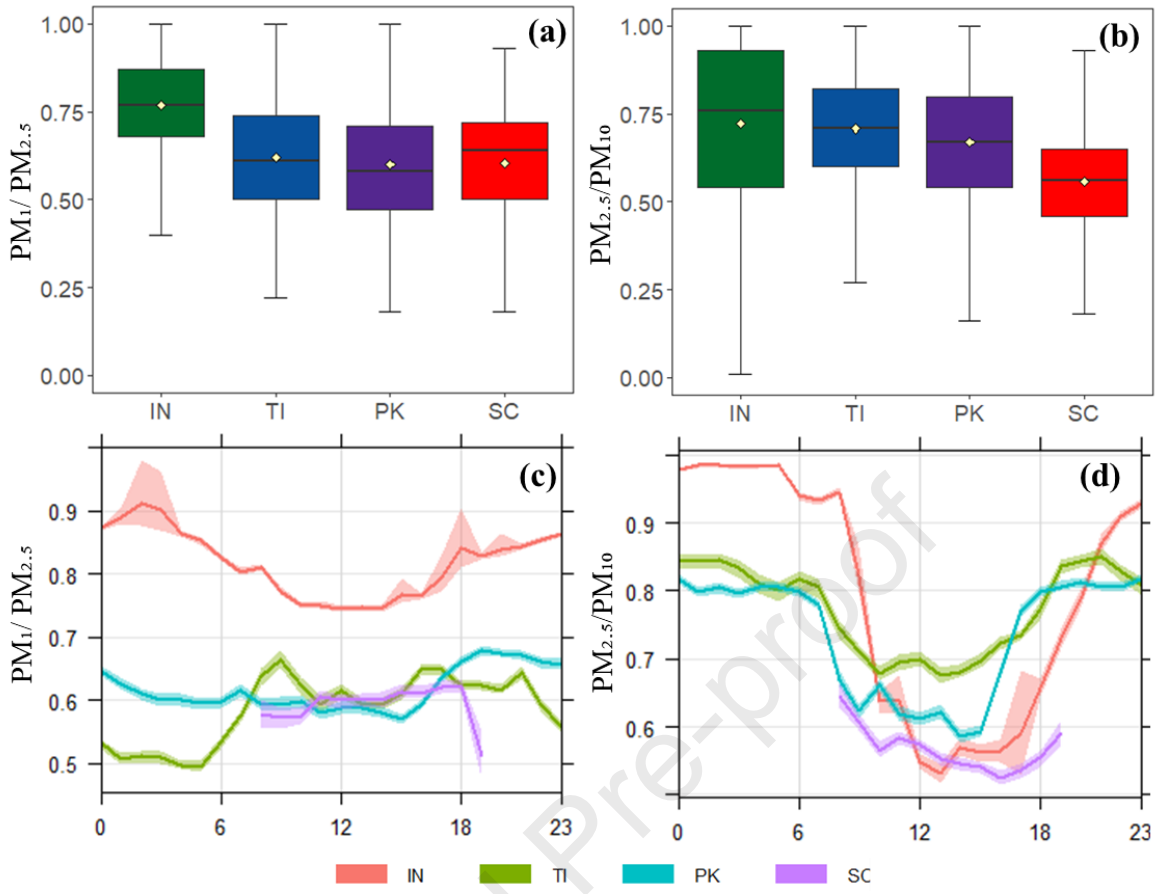

988

989 **Figure 4.** Boxplots showing the ratios of (a) $PM_1/PM_{2.5}$, (b) $PM_{2.5}/PM_{10}$ for the daytime (07:00-
990 19:00) and (c), (d) show their diurnal variation at IN, TI, PK and SC sites. The shaded area
991 indicates 95% confidence intervals.

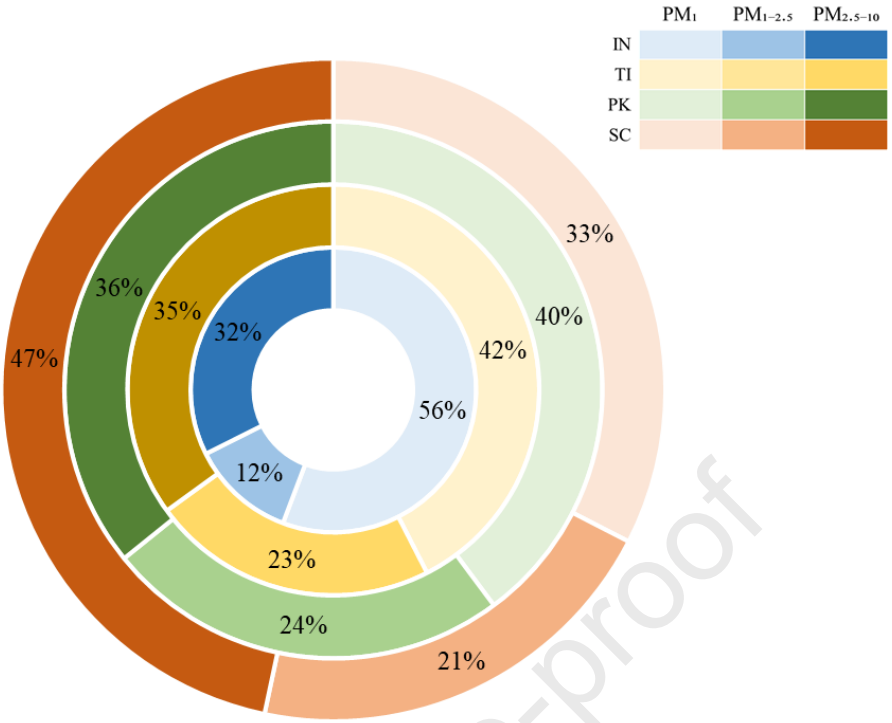

992

993 **Figure 5.** Pie charts showing the contribution of PM fractions (PM_1, $PM_{1\text{-}2.5}$, $PM_{2.5\text{-}10}$) to total

994 PM for IN, TI, PK and SC sites during the daytime.

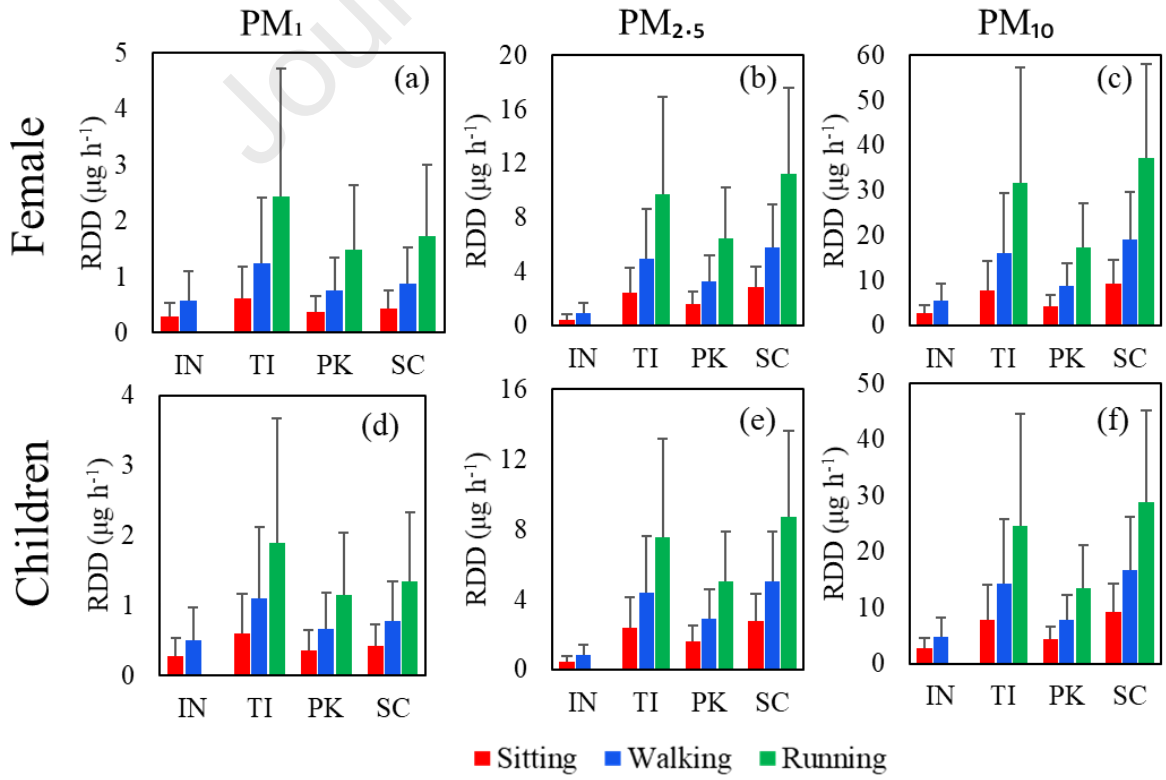

995

996 **Figure 6.** Respiratory Deposition Doses (RDD) for (a) PM_1, (b) $PM_{2.5}$, (c) PM_{10} for females
997 and (d), (e), (f) for children during three different activities at four different MEs.

998

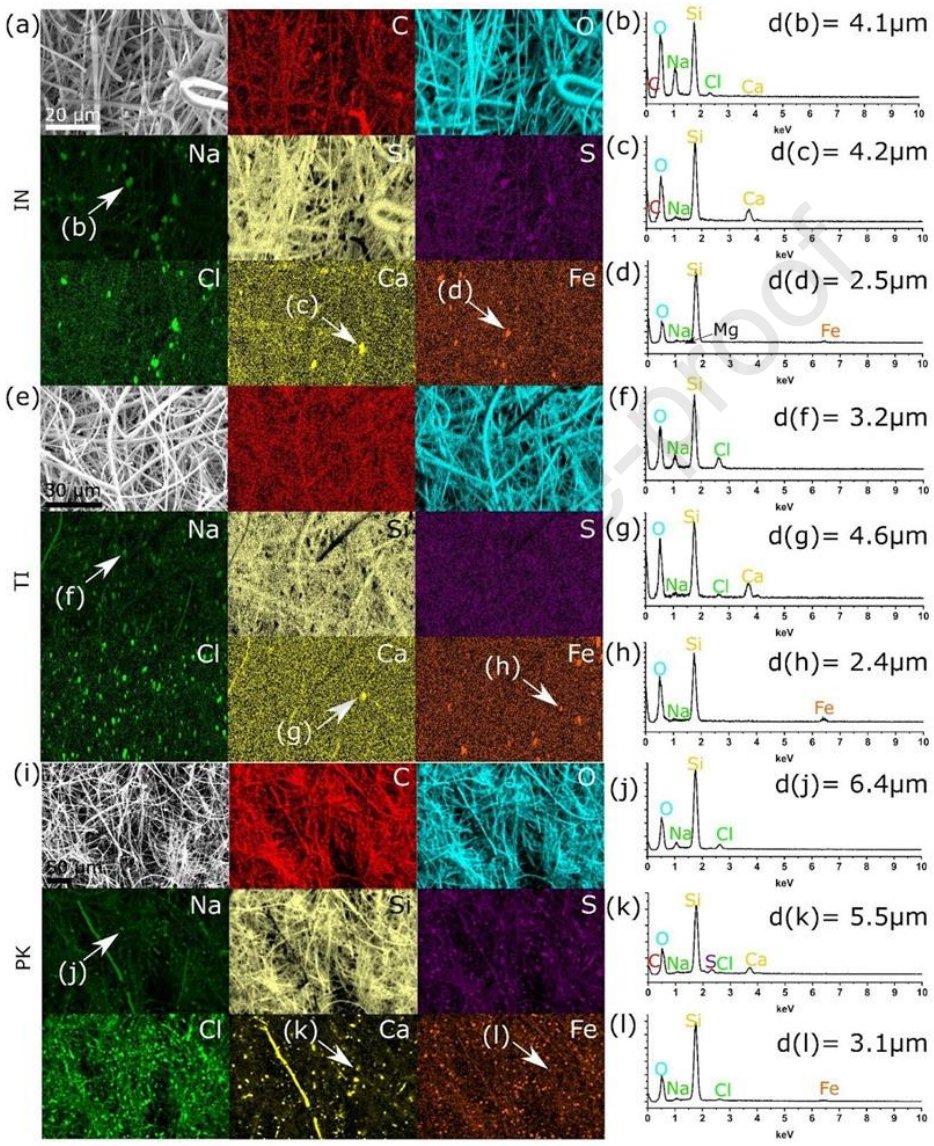

999

1000 **Figure 7.** ESEM images of $PM_{2.5}$ from (a) IN, with corresponding EDXS maps of C, O, Na,
1001 Si, S, Cl, Ca, Fe; spectra and Feret diameters of selected particles indicated by arrows (b), (c)
1002 and (d). Similarly (e-h) from TI and (i-l) from PK.

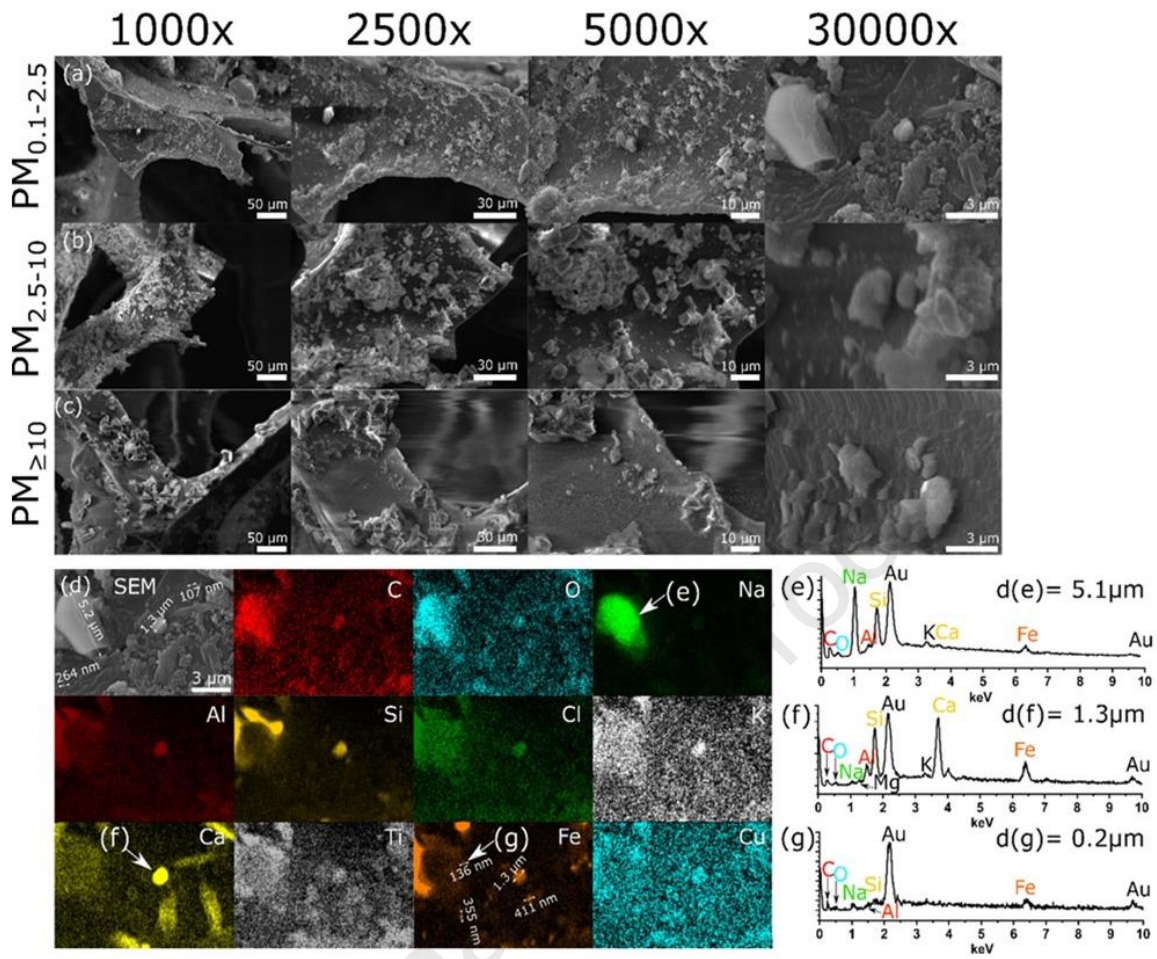

Figure 8. A series of SEM images at increasing magnifications showing PM collected on PUF at the SC site. The size fractions are (a) $PM_{0.1\text{-}2.5}$, (b) $PM_{2.5\text{-}10}$ and (c) $PM_{\geq 10}$. (d) High magnification SEM image of $PM_{0.1\text{-}2.5}$ with corresponding EDXS maps of C, O, Na, Al, Si, Cl, K, Ca, Ti, Fe and Cu. All maps are sorted by atomic number. (e), (f), (g) Characteristic EDX spectra and diameters of selected particles marked in (d).

Research Highlights

- Assessed air quality in four microenvironments; comparisons in exposure variations made.
- $PM_{2.5}$, $PM_{10,}$ PNC trend: traffic intersection, TI> street canyon, SC> park, PK> indoor, IN.
- Fine PM has smaller diurnal variation indoors compared to TI, PK and SC.
- Carcinogenic PAH do not breach relevant air quality standards in any microenvironment.
- RDD for all PM factions during running at PK is 39-53% lower compared to TI and SC.

Declaration of interests

☒ The authors declare that they have no known competing financial interests or personal relationships that could have appeared to influence the work reported in this paper.

☐The authors declare the following financial interests/personal relationships which may be considered as potential competing interests: